Lecture Recording

- **Note: These lectures will be recorded and posted onto the IMPRS website**

- Dear participants,

- We will record all lectures on "*Making sense of data: introduction to statistics for gravitational wave astronomy*", including possible Q&A after the presentation, and we will make the recordings publicly available on the IMPRS lecture website at:

  - ✍ https://imprs-gw-lectures.aei.mpg.de/2023-making-sense-of-data/

- By participating in this Zoom meeting, you are giving your explicit consent to the recording of the lecture and the publication of the recording on the course website.

Making sense of data: introduction to statistics for gravitational wave astronomy

Part II: Bayesian statistics

Lecture 3: Examples of Bayesian statistics in GW data analysis

AEI IMPRS Lecture Course

Alexandre Toubiana atoubiana@aei.mpg.de

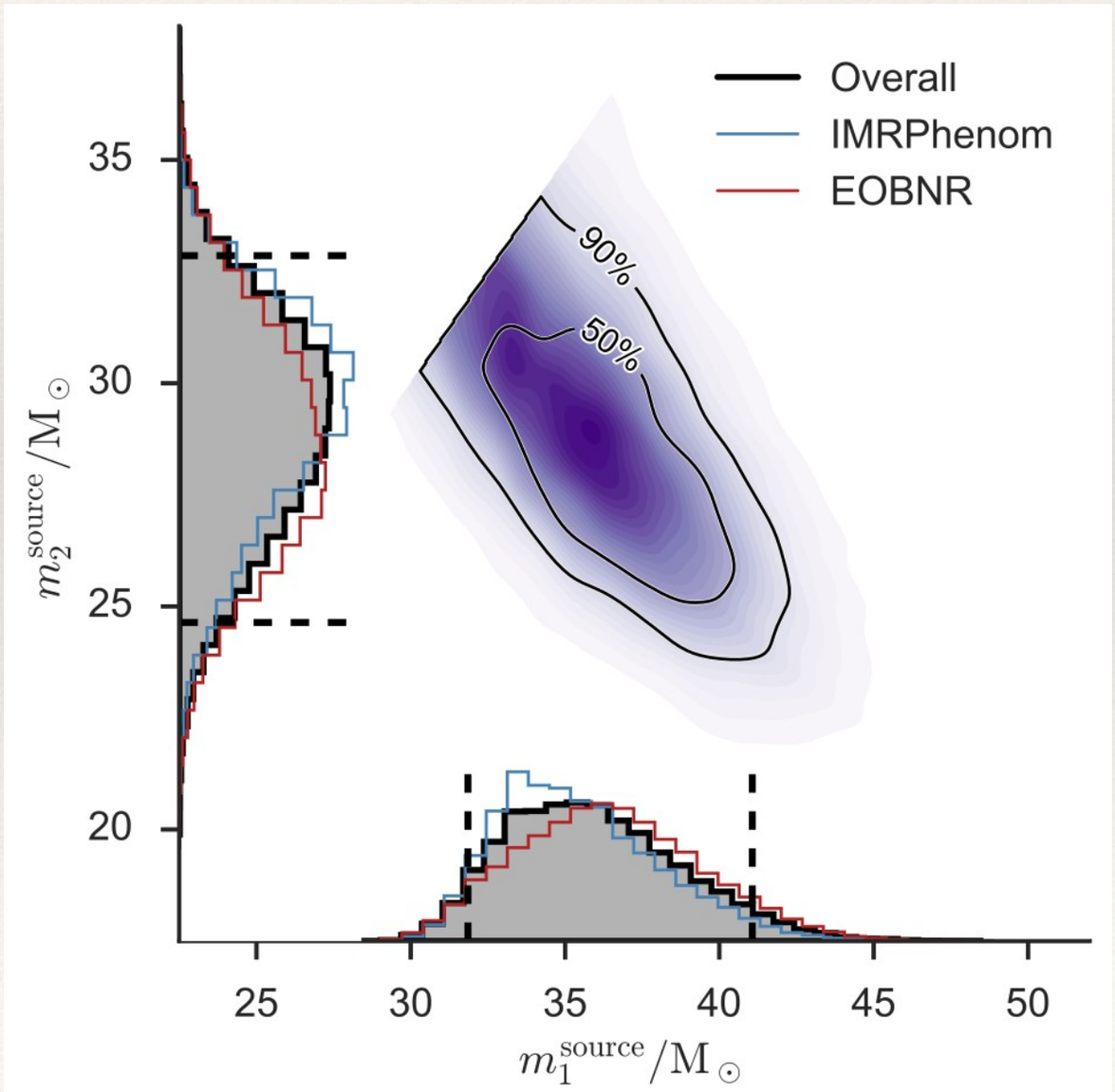

Parameter Estimation in the LVK

LIGO Parameter Estimation

- LIGO parameter estimation uses Bayesian methods. Results are quoted as posterior distributions, or posterior median values and credible intervals.
- Mix samples from IMRPhenomXHM and SEOBNRv4HM. See arXiv:2309.14473 for an analysis with NRSur7dq4. It will be included in O4 when possible.
- Results are presented in the public catalogues released by the LVK. So far GWTC-1 (arxiv:1811.12907), GWTC-2 (arxiv:2010.14527) and GWTC-3 (arxiv:2111.03606). O4 is ongoig. Also independent catalogues (Nitz et al., APJ 2023, Olsen et al., PRD 2022, Mehta et al., arXiv:2311.0606).
- Individual event results can be found on GWOSC. Other LVK analyses (tests of GR, population, cosmology ...) are provided on Zenodo.

Event	$m_1/M_\odot$	$m_2/M_\odot$	$\mathcal{M}/M_\odot$	$\chi_{\rm eff}$	$M_f/M_\odot$	a_f	$E_{\rm rad}/(M_\odot c^2)$	$\ell_{\rm peak}/({\rm erg\,s^{-1}})$	$d_L/{\rm Mpc}$	z	$\Delta\Omega/{\rm deg}^2$
GW150914	$35.6^{+4.7}_{-3.1}$	$30.6^{+3.0}_{-4.4}$	$28.6^{+1.7}_{-1.5}$	$-0.01^{+0.12}_{-0.13}$	$63.1^{+3.4}_{-3.0}$	$0.69^{+0.05}_{-0.04}$	$3.1^{+0.4}_{-0.4}$	$3.6^{+0.4}_{-0.4}\times10^{56}$	440^{+150}_{-170}	$0.09^{+0.03}_{-0.03}$	182
GW151012	$23.2^{+14.9}_{-5.5}$	$13.6^{+4.1}_{-4.8}$	$15.2^{+2.1}_{-1.2}$	$0.05^{+0.31}_{-0.20}$	$35.6^{+10.8}_{-3.8}$	$0.67^{+0.13}_{-0.11}$	$1.6^{+0.6}_{-0.5}$	$3.2^{+0.8}_{-1.7}\times10^{56}$	1080^{+550}_{-490}	$0.21^{+0.09}_{-0.09}$	1523
GW151226	$13.7^{+8.8}_{-3.2}$	$7.7^{+2.2}_{-2.5}$	$8.9^{+0.3}_{-0.3}$	$0.18^{+0.20}_{-0.12}$	$20.5^{+6.4}_{-1.5}$	$0.74^{+0.07}_{-0.05}$	$1.0^{+0.1}_{-0.2}$	$3.4^{+0.7}_{-1.7}\times10^{56}$	450^{+180}_{-190}	$0.09^{+0.04}_{-0.04}$	1033
GW170104	$30.8^{+7.3}_{-5.6}$	$20.0^{+4.9}_{-4.6}$	$21.4^{+2.2}_{-1.8}$	$-0.04^{+0.17}_{-0.21}$	$48.9^{+5.1}_{-4.0}$	$0.66^{+0.08}_{-0.11}$	$2.2^{+0.5}_{-0.5}$	$3.3^{+0.6}_{-1.0}\times10^{56}$	990^{+440}_{-430}	$0.20^{+0.08}_{-0.08}$	921
GW170608	$11.0^{+5.5}_{-1.7}$	$7.6^{+1.4}_{-2.2}$	$7.9^{+0.2}_{-0.2}$	$0.03^{+0.19}_{-0.07}$	$17.8^{+3.4}_{-0.7}$	$0.69^{+0.04}_{-0.04}$	$0.9^{+0.0}_{-0.1}$	$3.5^{+0.4}_{-1.3}\times10^{56}$	320^{+120}_{-110}	$0.07^{+0.02}_{-0.02}$	392
GW170729	$50.2^{+16.2}_{-10.2}$	$34.0^{+9.1}_{-10.1}$	$35.4^{+6.5}_{-4.8}$	$0.37^{+0.21}_{-0.25}$	$79.5^{+14.7}_{-10.2}$	$0.81^{+0.07}_{-0.13}$	$4.8^{+1.7}_{-1.7}$	$4.2^{+0.9}_{-1.5}\times10^{56}$	2840^{+1400}_{-1360}	$0.49^{+0.19}_{-0.21}$	1041
GW170809	$35.0^{+8.3}_{-5.9}$	$23.8^{+5.1}_{-5.2}$	$24.9^{+2.1}_{-1.7}$	$0.08^{+0.17}_{-0.17}$	$56.3^{+5.2}_{-3.8}$	$0.70^{+0.08}_{-0.09}$	$2.7^{+0.6}_{-0.6}$	$3.5^{+0.6}_{-0.9}\times10^{56}$	1030^{+320}_{-390}	$0.20^{+0.05}_{-0.07}$	308
GW170814	$30.6^{+5.6}_{-3.0}$	$25.2^{+2.8}_{-4.0}$	$24.1^{+1.4}_{-1.1}$	$0.07^{+0.12}_{-0.12}$	$53.2^{+3.2}_{-2.4}$	$0.72^{+0.07}_{-0.05}$	$2.7^{+0.4}_{-0.3}$	$3.7^{+0.4}_{-0.5}\times10^{56}$	600^{+150}_{-220}	$0.12^{+0.03}_{-0.04}$	87
GW170817	$1.46^{+0.12}_{-0.10}$	$1.27^{+0.09}_{-0.09}$	$1.186^{+0.001}_{-0.001}$	$0.00^{+0.02}_{-0.01}$	≤ 2.8	≤ 0.89	≥ 0.04	$\geq 0.1\times10^{56}$	40^{+7}_{-15}	$0.01^{+0.00}_{-0.00}$	16
GW170818	$35.4^{+7.5}_{-4.7}$	$26.7^{+4.3}_{-5.2}$	$26.5^{+2.1}_{-1.7}$	$-0.09^{+0.18}_{-0.21}$	$59.4^{+4.9}_{-3.8}$	$0.67^{+0.07}_{-0.08}$	$2.7^{+0.5}_{-0.5}$	$3.4^{+0.5}_{-0.7}\times10^{56}$	1060^{+420}_{-380}	$0.21^{+0.07}_{-0.07}$	39
GW170823	$39.5^{+11.2}_{-6.7}$	$29.0^{+6.7}_{-7.8}$	$29.2^{+4.6}_{-3.6}$	$0.09^{+0.22}_{-0.26}$	$65.4^{+10.1}_{-7.4}$	$0.72^{+0.09}_{-0.12}$	$3.3^{+1.0}_{-0.9}$	$3.6^{+0.7}_{-1.1}\times10^{56}$	1940^{+970}_{-900}	$0.35^{+0.15}_{-0.15}$	1666

LVK, PRX 2019

LVK PE codes

- In O1 and O2, LVK parameter estimation used the *LALInference* code. This includes two separate algorithms:
  - *LALInferenceMCMC*: A Markov Chain Monte Carlo code based on the Metropolis-Hastings algorithm. Proposal distributions are tuned to features of the likelihood expected for CBC inspirals.
  - *LALInferenceNest*: A bespoke nested sampling algorithm. New live points are drawn by evolving mini-MCMC chains until an independent point is obtained.
- During O3 a new software package, *Bilby*, was introduced (also with a parallel implementation, *parallel bilby*). The sampling algorithms in *Bilby* are not bespoke. Instead it uses freely available packages such as *dynesty*. LALInference was also used in O3, alongside *Bilby*.
- For O4, Bilby should be the primary inference package. DINGO is currently under review.

LVK PE results: examples

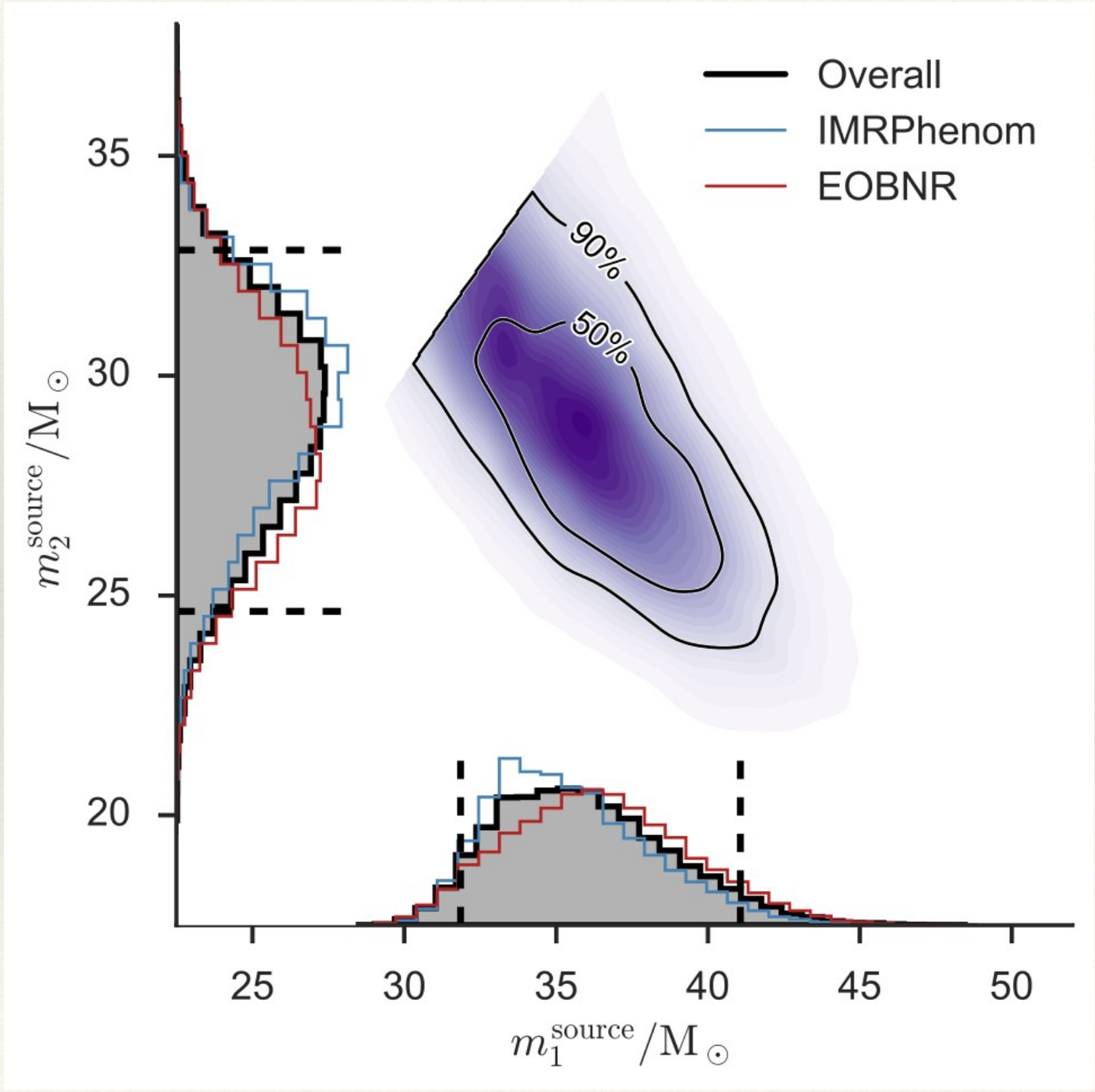

LVK, PRL 2016

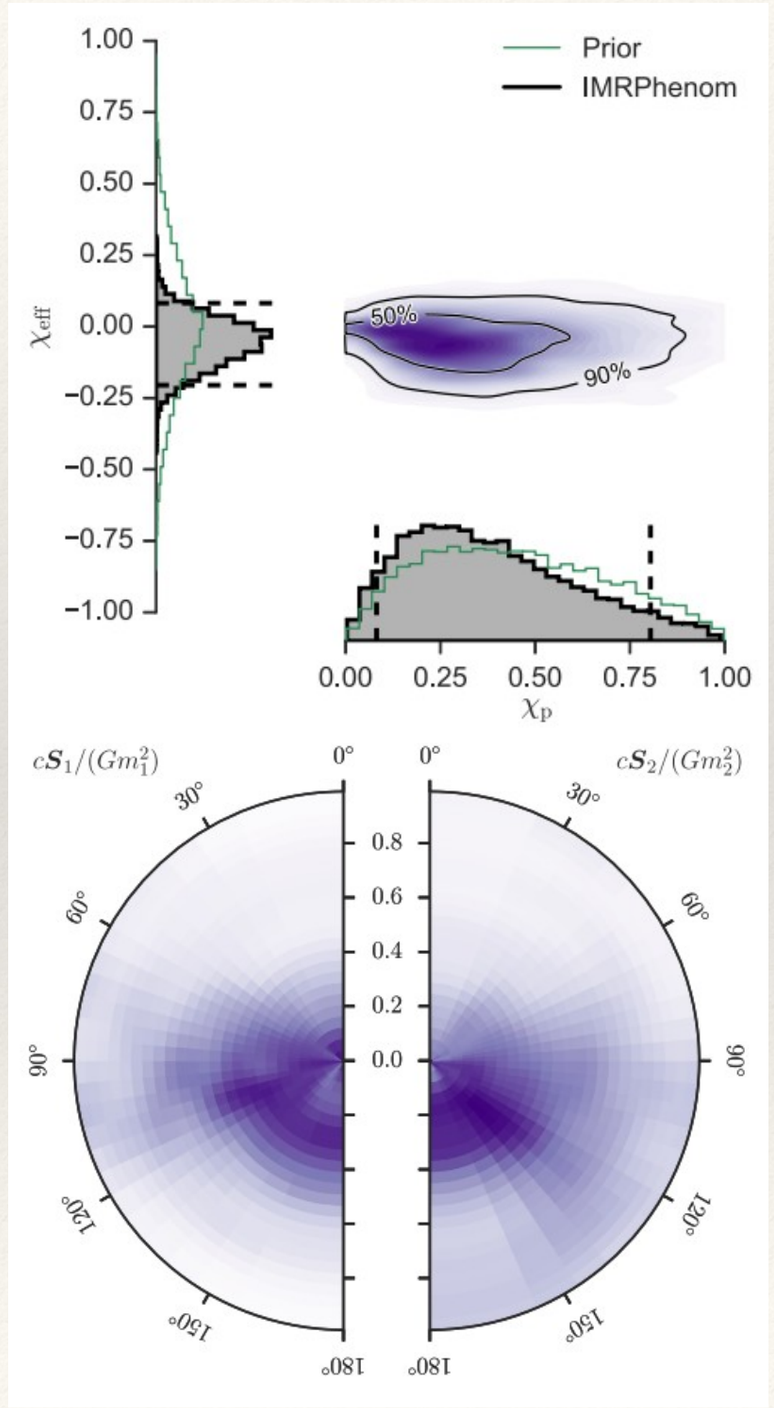

LVK PE results: examples

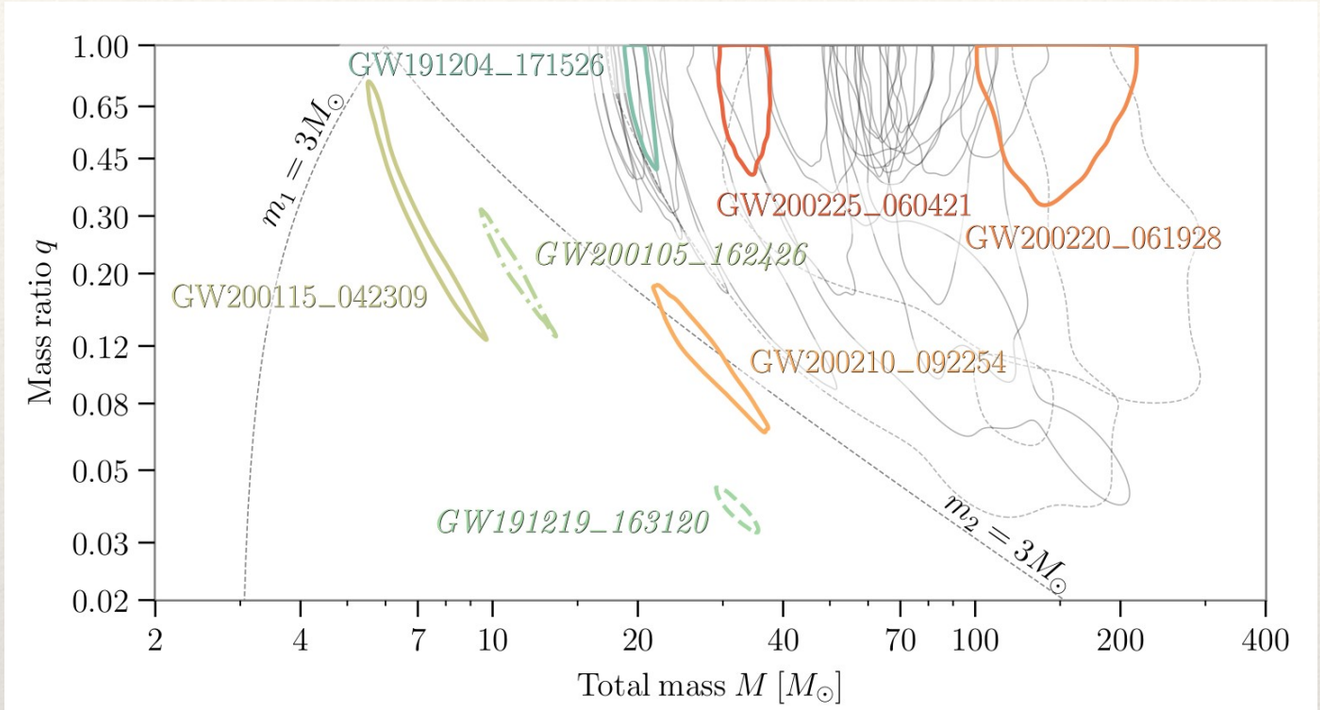

- Several NSBH candidates
- Evidence for spinning BHs

LVK, 2111.03606

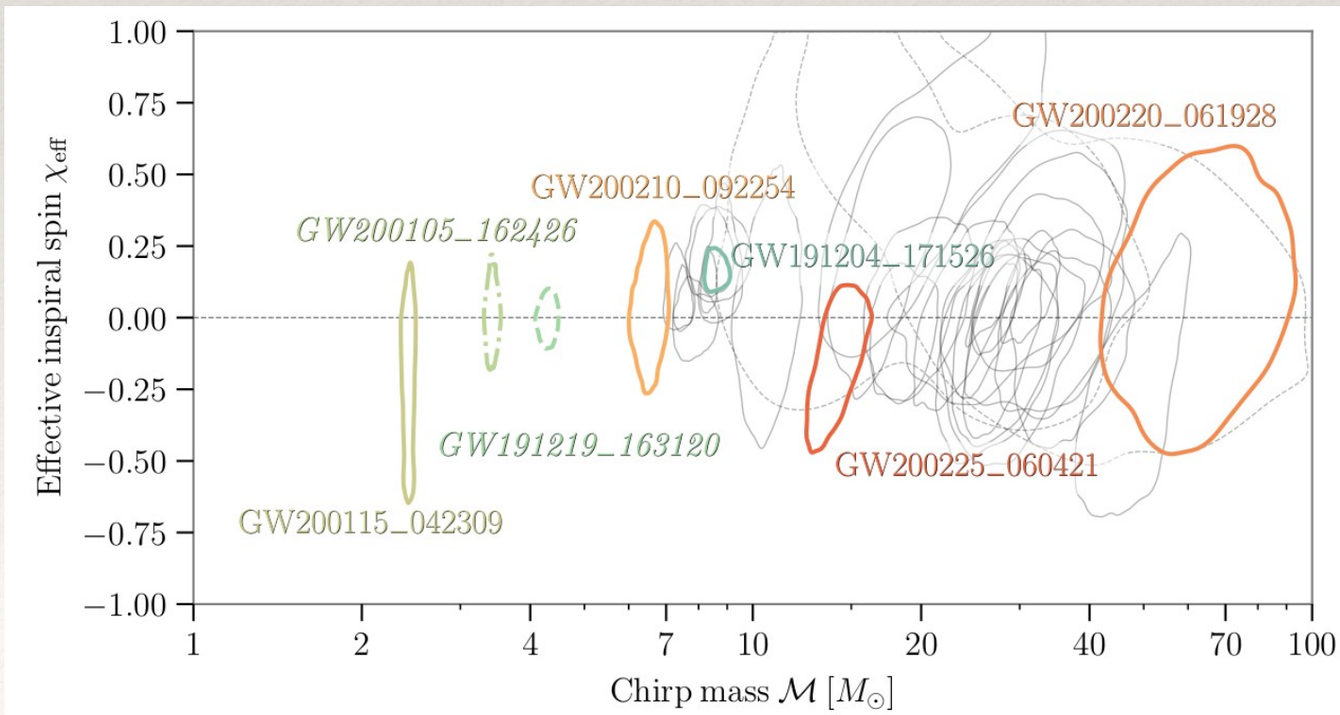

LVK PE results: examples

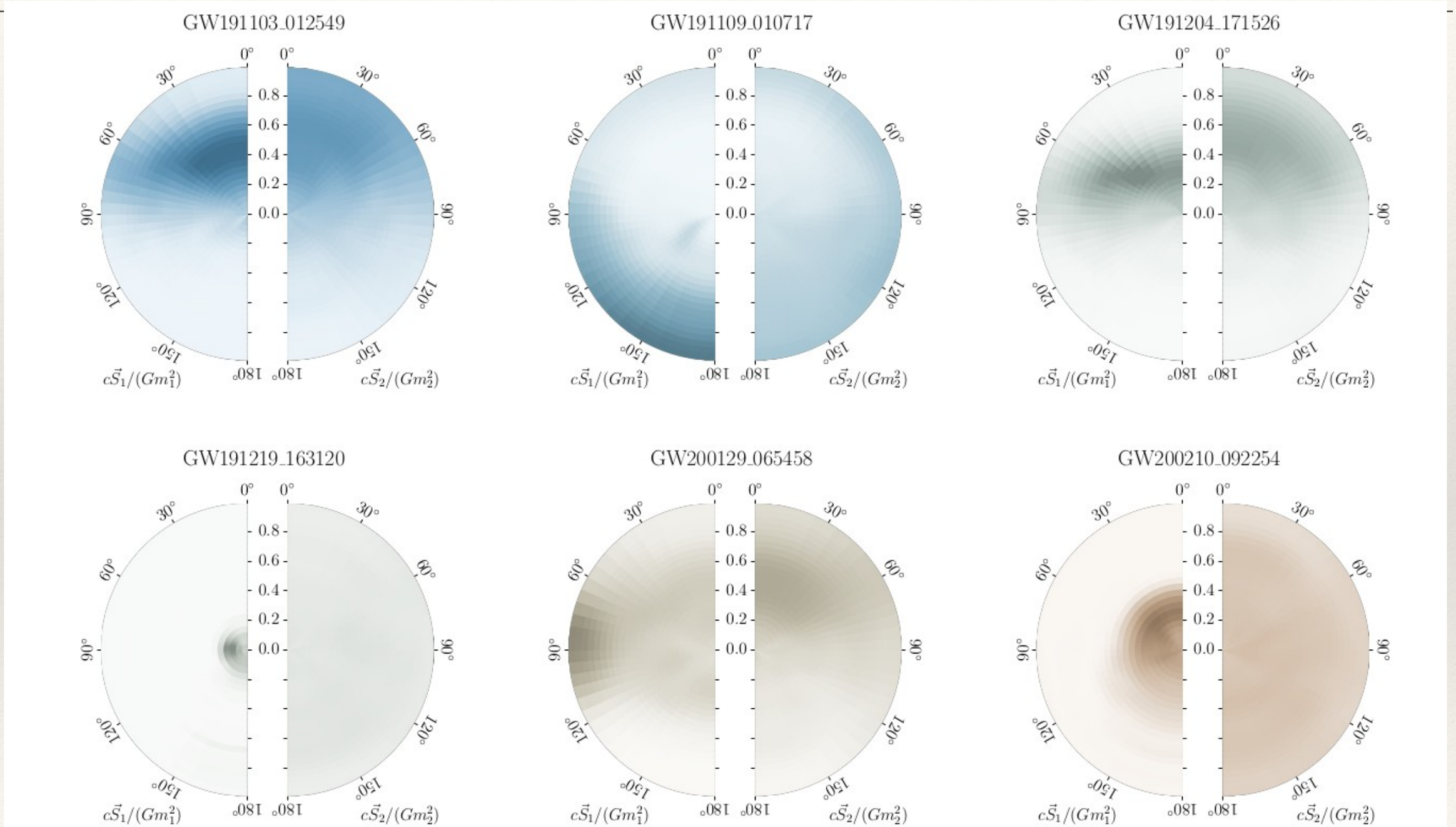

LVK, 2111.03606

LVK PE results: examples

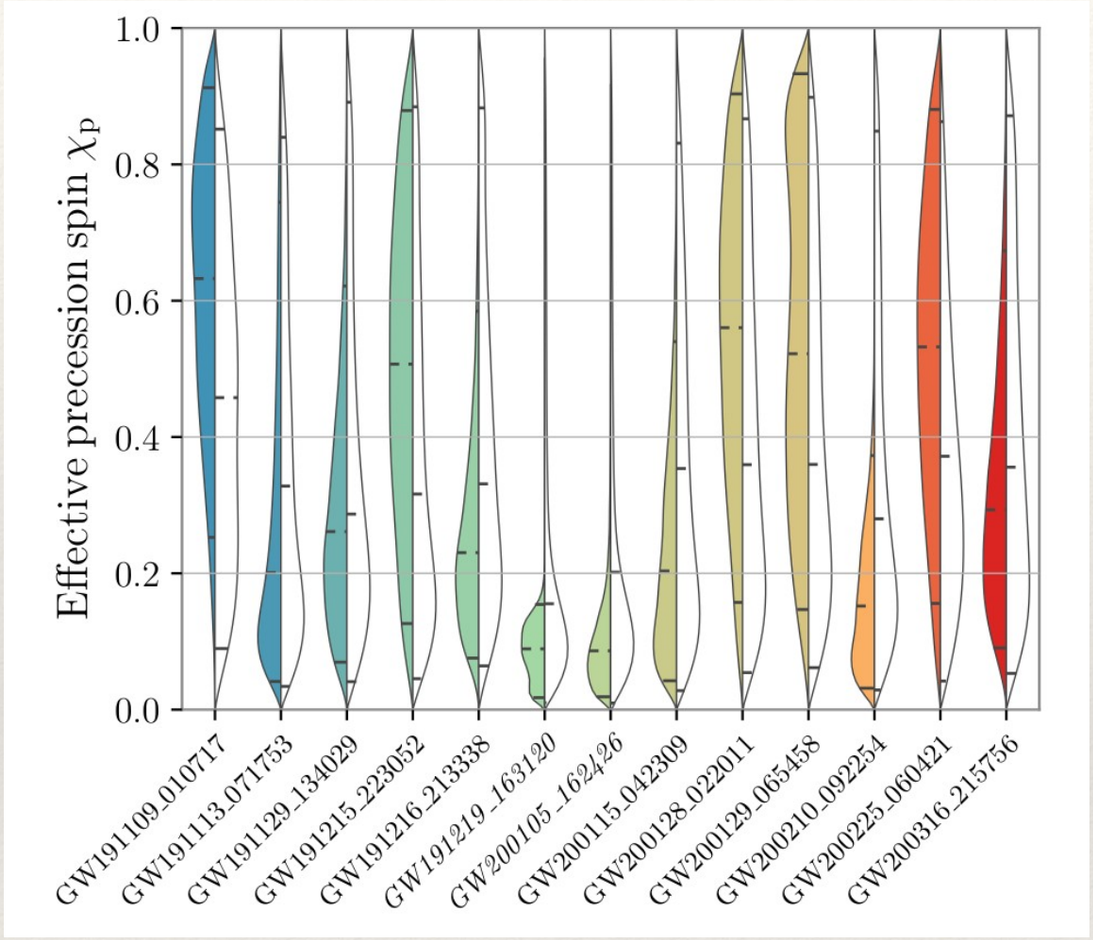

- Little difference between prior and posterior
- GW200129_065458 has $\chi_p = 0.52^{+0.41}_{-0.38}$
- High SNR (~27) and the results changes significantly between IMRPhenomXHM and SEOBNRv4HM.
  NRSur7dq4 in better agreement with IMRPhenomXHM.

LVK, 2111.03606

Islam et al., 2309.14473

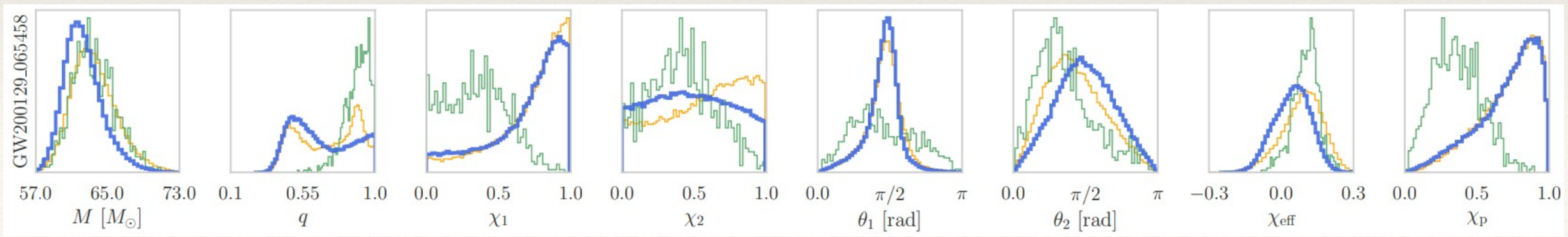

LVK PE results: examples

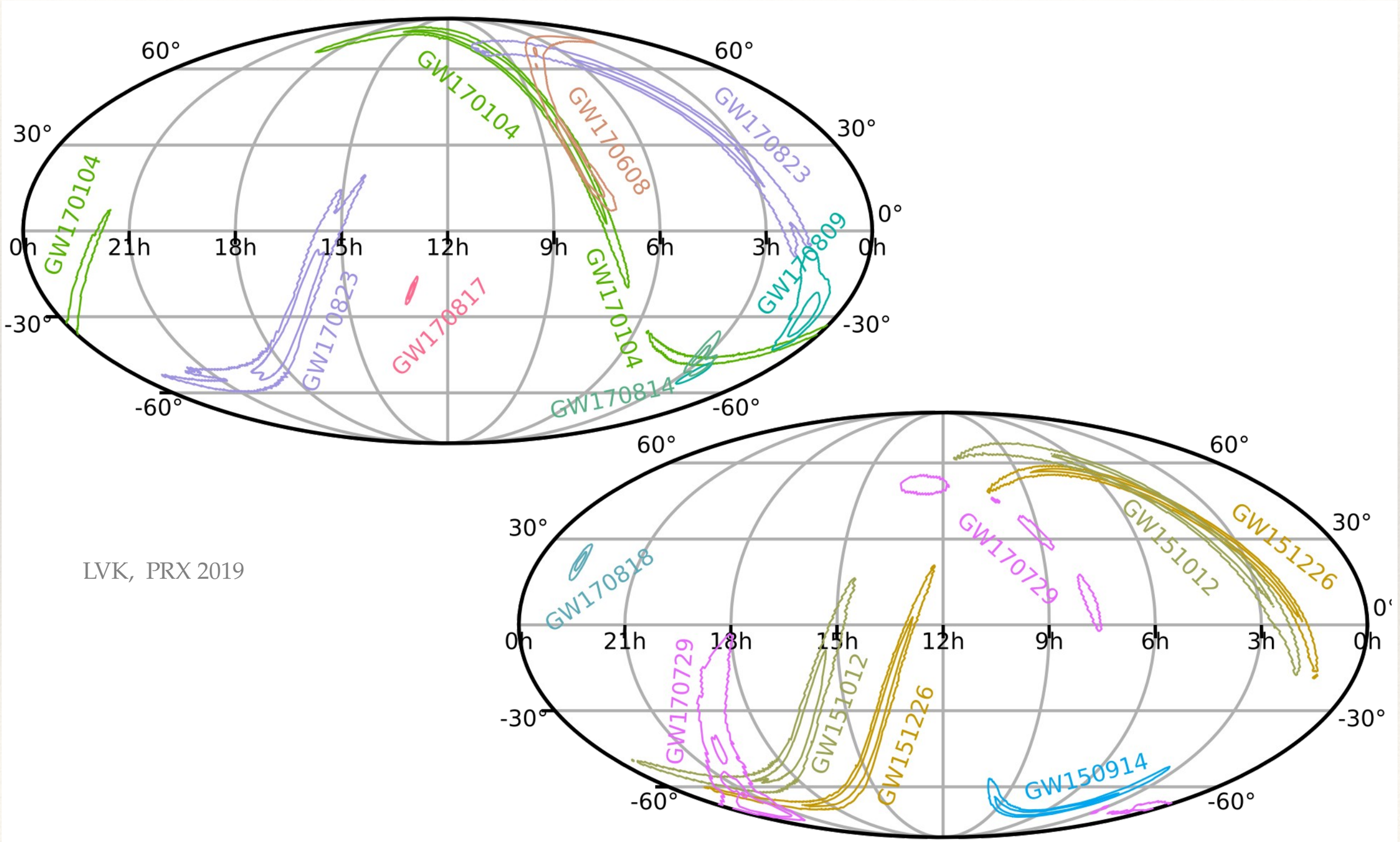

LVK, PRX 2019

Tests of GR

Parametrised tests

- So far very few theoretically motivated non-GR waveforms are available
- We have to resort to parametrised tests, in the inspiral and/or merger-ringdown:

			$\lvert\beta\rvert$		Example theory constraints			
Theoretical mechanism	GR pillar	PN	GW150914	GW151226	Repr. parameters	GW150914	GW151226	Current bounds
Scalar field activation	SEP	-1	$\mathbf{1.6\times10^{-4}}$	$\mathbf{4.4\times10^{-5}}$	$\sqrt{\lvert\alpha_{\rm EdGB}\rvert}$ [km]	...	...	10^7 [60], 2 [61–63]
					$\lvert\dot{\phi}\rvert$ [1/sec]	...	...	10^{-6} [64]
Scalar field activation	SEP, PI	$+2$	$\mathbf{1.3\times10^{1}}$	$\mathbf{4.1}$	$\sqrt{\lvert\alpha_{\rm dCS}\rvert}$ [km]	...	...	10^8 [65,66]
Vector field activation	SEP, LI	0	$\mathbf{7.2\times10^{-3}}$	$\mathbf{3.4\times10^{-3}}$	(c_+, c_-)	$(\mathbf{0.9}, \mathbf{2.1})$	$(\mathbf{0.8}, \mathbf{1.1})$	(0.03,0.003) [67,68]
					$(\beta_{\rm KG}, \lambda_{\rm KG})$	$(\mathbf{0.42}, -)$	$(\mathbf{0.40}, -)$	(0.005,0.1) [67,68]
Extra dimensions	4D	-4	$\mathbf{9.1\times10^{-9}}$	$\mathbf{9.1\times10^{-11}}$	ℓ [μm]	$\mathbf{5.4\times10^{10}}$	$\mathbf{2.0\times10^{9}}$	10–10^3 [69–73]
Time-varying G	SEP	-4	$\mathbf{9.1\times10^{-9}}$	$\mathbf{9.1\times10^{-11}}$	$\lvert\dot{G}\rvert$ [10^{-12}/yr]	$\mathbf{5.4\times10^{18}}$	$\mathbf{1.7\times10^{17}}$	0.1–1 [74–78]
Massive graviton	$m_g=0$	$+1$	$\mathbf{1.3\times10^{-1}}$	$\mathbf{8.9\times10^{-2}}$	m_g [eV]	$\mathbf{10^{-22}}$ [19]	$\mathbf{10^{-22}}$ [5]	10^{-29}–10^{-18} [79–83]
Mod. disp. rel.	LI	$+4.75$	$\mathbf{1.1\times10^{2}}$	$\mathbf{2.6\times10^{2}}$	E_*^{-1} [eV^{-1}] (time)	$\mathbf{5.8\times10^{-27}}$	$\mathbf{3.3\times10^{-26}}$	...
(*multifractional*)					E_*^{-1} [eV^{-1}] (space)	$\mathbf{1.0\times10^{-26}}$	$\mathbf{5.7\times10^{-26}}$	3.9×10^{-53} [84]
Mod. disp. rel.	LI	$+5.5$	$\mathbf{1.4\times10^{2}}$	$\mathbf{4.3\times10^{2}}$	$\eta_{\rm dsrt}/L_{\rm Pl}>0$	$\mathbf{1.3\times10^{22}}$	$\mathbf{3.8\times10^{22}}$	...
(*modified special rel.*)					$\eta_{\rm dsrt}/L_{\rm Pl}<0$			2.1×10^{-7} [84]
Mod. disp. rel.	4D	$+7$	$\mathbf{5.3\times10^{2}}$	$\mathbf{2.4\times10^{3}}$	$\alpha_{\rm edt}/L_{\rm Pl}^2>0$	$\mathbf{5.5\times10^{62}}$	$\mathbf{2.5\times10^{63}}$	2.7×10^{2} [84]
(*extra dim.*)					$\alpha_{\rm edt}/L_{\rm Pl}^2<0$			...
		$+4$	...	...	$\overset{\circ}{k}{}^{(4)}_{(I)}>0$	...	...	6.1×10^{-17} [84,85]
					$\overset{\circ}{k}{}^{(4)}_{(I)}<0$	$\mathbf{0.64}$	$\mathbf{19}$	...
Mod. disp. rel.	LI	$+5.5$	$\mathbf{1.4\times10^{2}}$	$\mathbf{4.3\times10^{2}}$	$\overset{\circ}{k}{}^{(5)}_{(V)}>0$ [cm]	$\mathbf{1.7\times10^{-12}}$ [86]	$\mathbf{3.1\times10^{-11}}$	1.7×10^{-40} [84,85]
(*standard model ext.*)					$\overset{\circ}{k}{}^{(5)}_{(V)}<0$ [cm]			...
		$+7$	$\mathbf{5.3\times10^{2}}$	$\mathbf{2.4\times10^{3}}$	$\overset{\circ}{k}{}^{(6)}_{(I)}>0$ [cm^2]	$\mathbf{7.2\times10^{-4}}$	$\mathbf{3.3\times10^{-3}}$	3.5×10^{-64} [84,85]
					$\overset{\circ}{k}{}^{(6)}_{(I)}<0$ [cm^2]			...
Mod. disp. rel.	LI	$+7$	$\mathbf{5.3\times10^{2}}$	$\mathbf{2.4\times10^{3}}$	$\kappa_{\rm hl}^4\mu_{\rm hl}^2$ [1/eV^2]	$\mathbf{1.5\times10^{6}}$	$\mathbf{6.9\times10^{6}}$	...
(*Hořava-Lifshitz*)								
Mod. disp. rel.	LI	$+4$	...	...	c_+	$\mathbf{0.7}$ [87]	$\mathbf{0.998}$	0.03 [67,68]
(*Lorentz violation*)								

Yunes et al., PRD 2016

Inspiral tests: propagation

- Assume modified dispersion relation: $E^2 = p^2c^2 + A_\alpha p^\alpha c^\alpha$
- Leads to deviation in the phase:

$$\delta\varphi = -\frac{\pi^{2-\alpha}}{1-\alpha}\frac{D_\alpha^{1-\alpha}}{(1+Z)^{1-\alpha}}\frac{A_\alpha}{(hc)^2}(\pi\mathcal{M}_c f)^{\alpha-1}$$

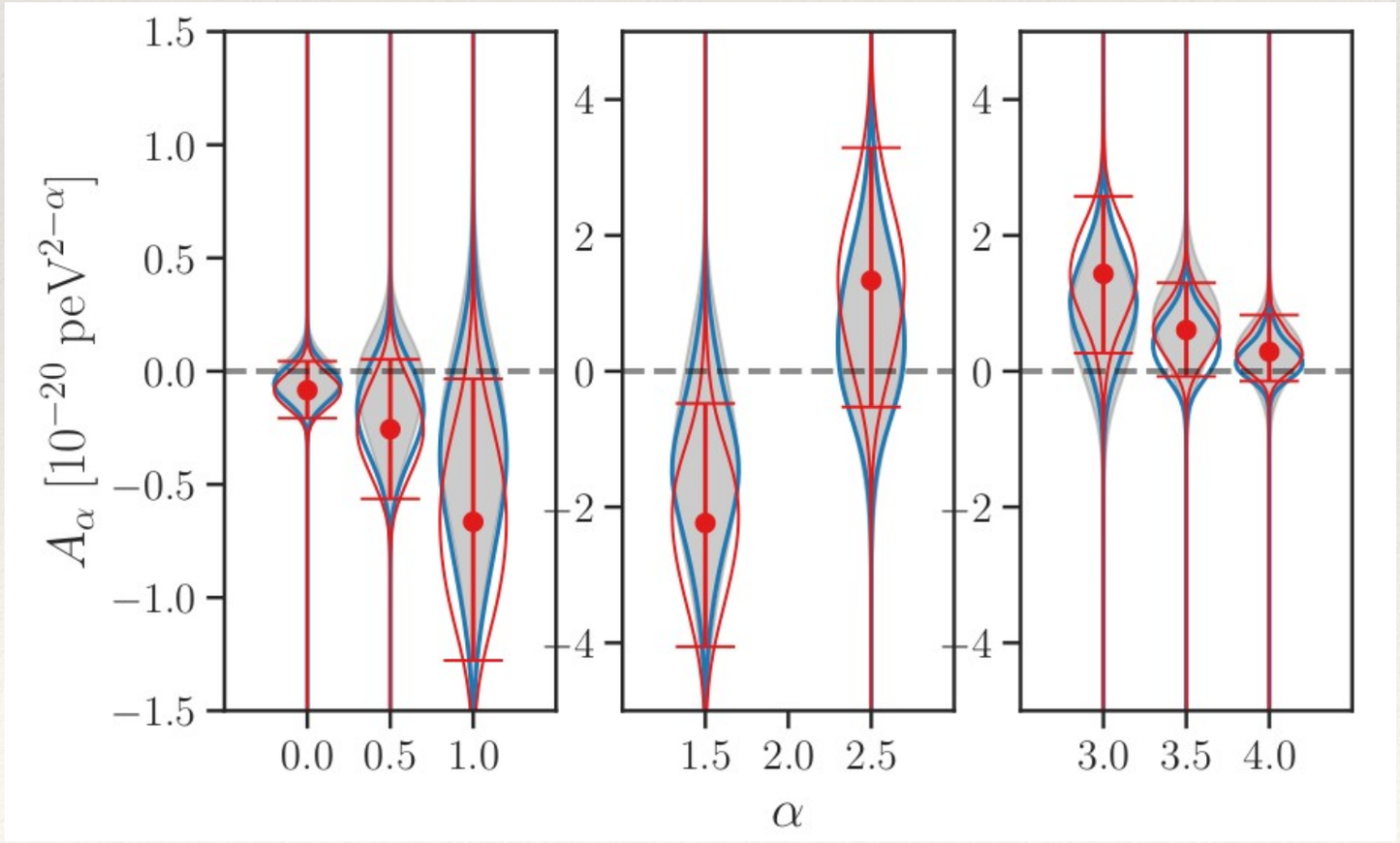

LVK, 2112.06861

Inspiral tests: generation

- Add deviations to the different PN orders to account for mechanisms that modify the generation of GWs
- Combine hierarchically or assuming unique value for each

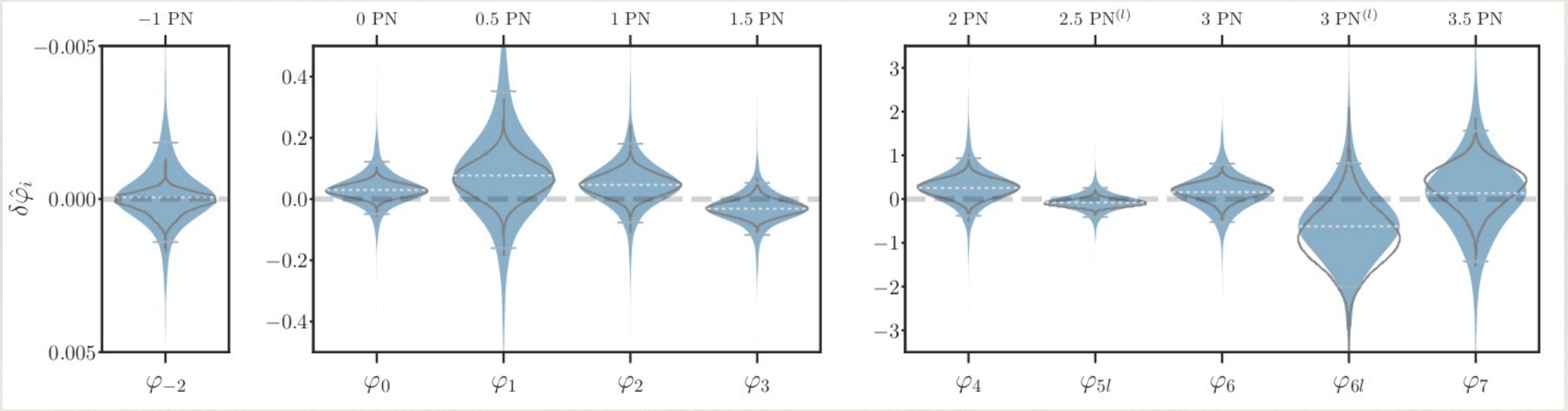

LVK, 2112.06861

IMR consistency test

- Split the signal in two and estimate final mass and final spin from each portion

$$\frac{\Delta M_f}{\bar{M}_f} = 2\frac{M_f^{\rm insp} - M_f^{\rm postinsp}}{M_f^{\rm insp} + M_f^{\rm postinsp}}$$

$$\frac{\Delta \chi_f}{\bar{\chi}_f} = 2\frac{\chi_f^{\rm insp} - \chi_f^{\rm postinsp}}{\chi_f^{\rm insp} + \chi_f^{\rm postinsp}}$$

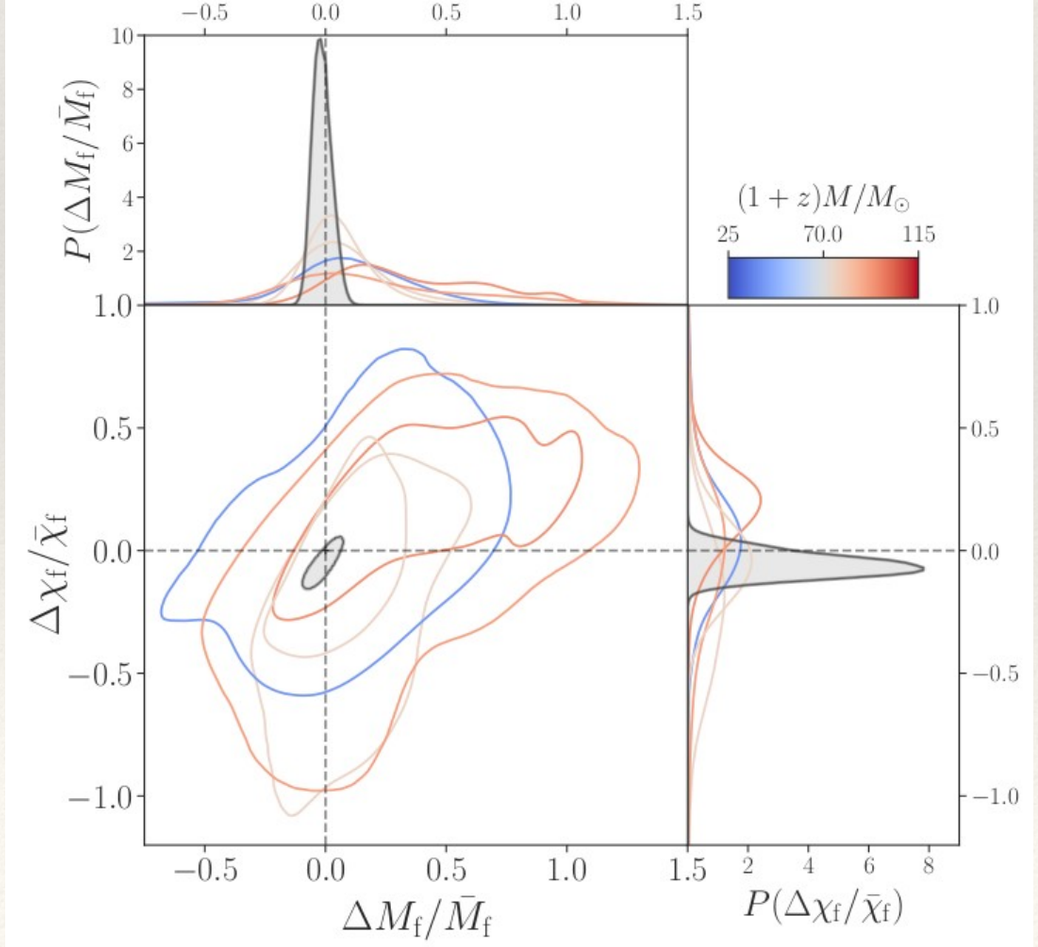

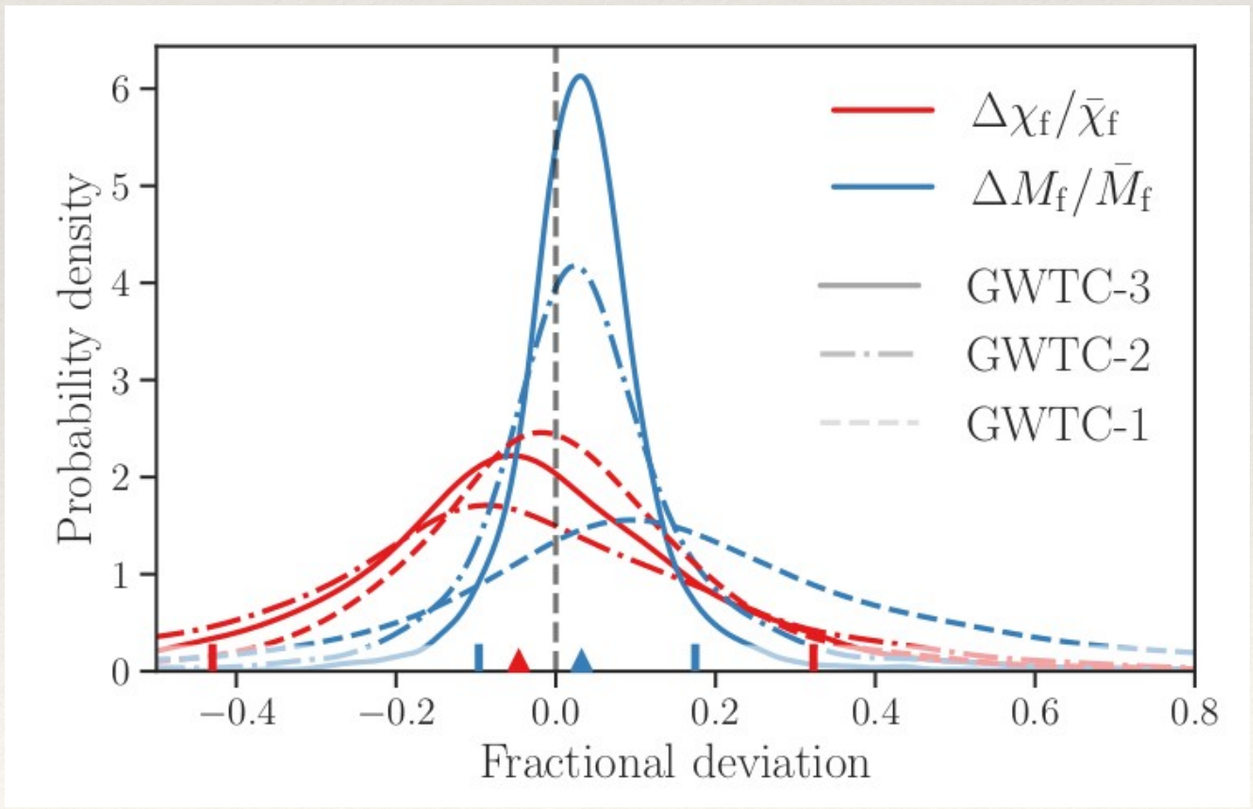

Ringdown

- pSEOBNR: fit the whole IMR signal and allow for deviations in the quasi-normal modes (QNMs):

$$f_{220} = f_{220,\mathrm{Kerr}}(1 + \delta f_{220}) \qquad \tau_{220} = \tau_{220,\mathrm{Kerr}}(1 + \delta\tau_{220})$$

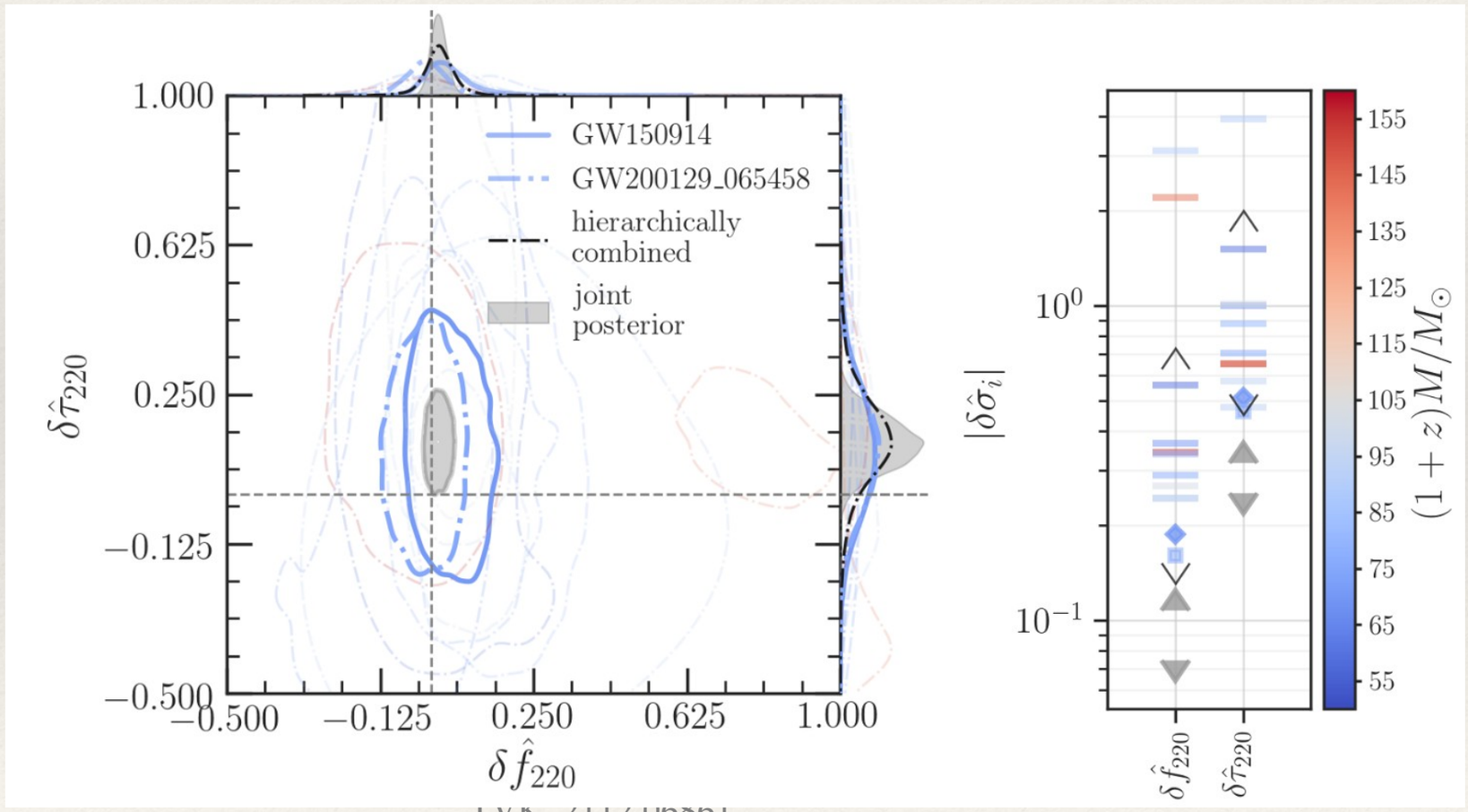

LVK, 2112.06861

- pSEOBNR has been extended to account for GR deviations in the merger part (Maggio et al., PRD 2023)

Cosmic variance

- Bias goes as $1/\sqrt{N_{\rm obs}}$ and standard deviation as $\sqrt{N_{\rm obs}}$, so we might favour non-GR because of our particular realisation of the Universe…
- Bootstrapping can be used to alleviate this

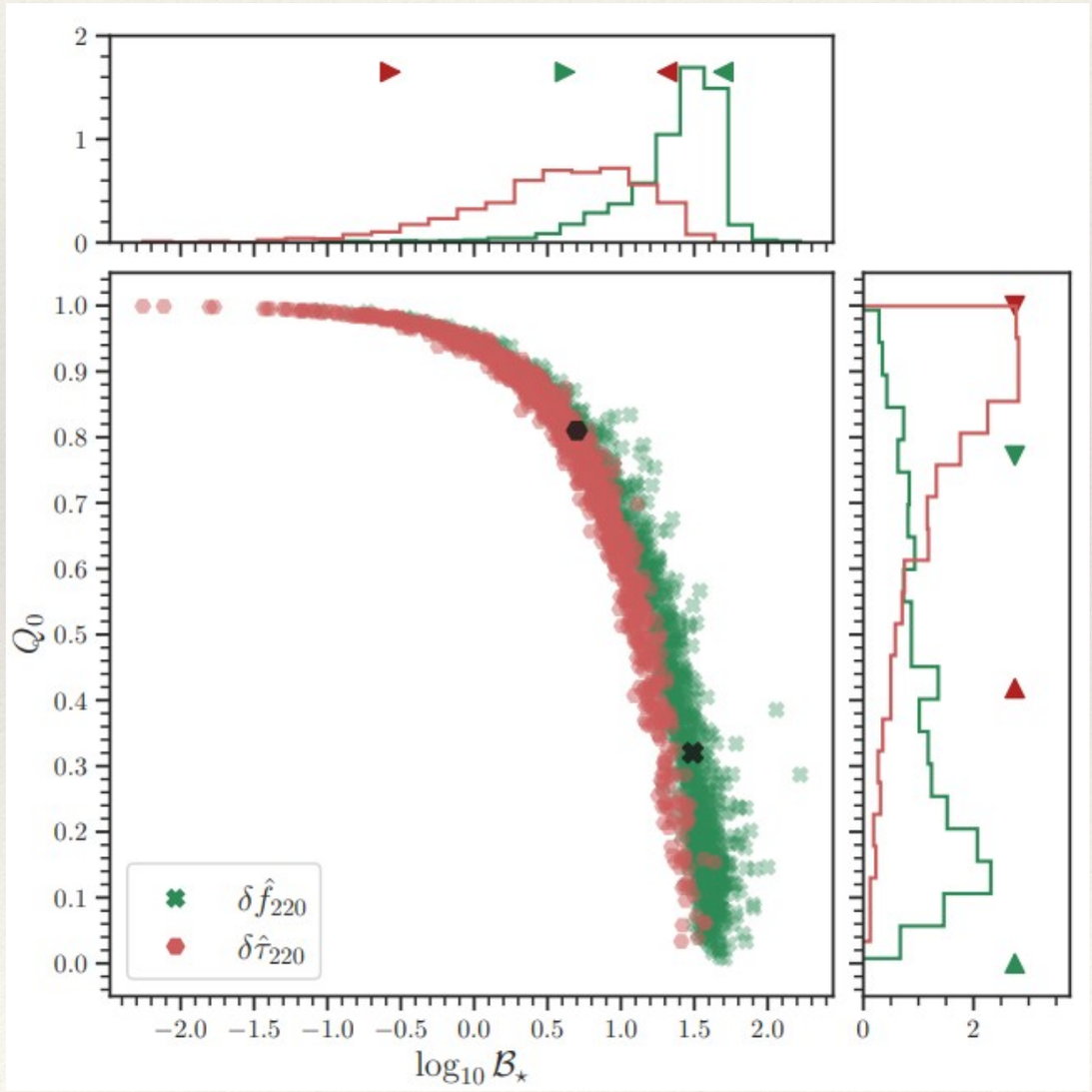

Pacilio et al., :2310.0381

Ringdown: spectroscopy

- Test the Kerr nature of the remnant. LVK uses PyRing

$$h = \sum_{\ell mn} A_{\ell mn} e^{-t/(\tau_{\ell mn}(M_f, a_f)(1+\delta\tau_{\ell mn}))} e^{i(2\pi f_{\ell mn}(M_f, a_f)(1+\delta f_{\ell mn})t + \varphi_{\ell mn})}$$

- Analysis done in time domain $\ln \mathcal{L} = -\frac{1}{2}(d(t_i) - h(\theta, t_i))C_{ij}^{-1}(d(t_j) - h(\theta, t_j))$
- Need to choose a starting time.

Event	Redshifted final mass $(1+z)M_f$ $[M_\odot]$				Final spin χ_f				Higher modes	Overtones	
	IMR	Kerr_{220}	Kerr_{221}	Kerr_{HM}	IMR	Kerr_{220}	Kerr_{221}	Kerr_{HM}	$\log_{10}\mathcal{B}^{\text{HM}}_{220}$	$\log_{10}\mathcal{B}^{221}_{220}$	$\log_{10}\mathcal{O}^{\text{modGR}}_{\text{GR}}$
GW191109_010717	$132.7^{+21.9}_{-13.8}$	$181.7^{+28.5}_{-30.6}$	$179.0^{+23.7}_{-21.7}$	$174.5^{+38.1}_{-30.1}$	$0.60^{+0.22}_{-0.19}$	$0.81^{+0.10}_{-0.24}$	$0.81^{+0.08}_{-0.14}$	$0.77^{+0.11}_{-0.21}$	−0.11	1.03	−0.27
GW191222_033537	$114.2^{+14.3}_{-11.7}$	$111.4^{+69.3}_{-29.7}$	$110.3^{+36.2}_{-23.8}$	$118.3^{+97.0}_{-46.2}$	$0.67^{+0.08}_{-0.10}$	$0.46^{+0.41}_{-0.41}$	$0.52^{+0.31}_{-0.43}$	$0.60^{+0.28}_{-0.66}$	0.08	−0.83	−0.20
GW200129_065458	$71.8^{+4.4}_{-3.9}$	$60.0^{+16.7}_{-8.9}$	$77.0^{+14.4}_{-14.2}$	$219.1^{+110.4}_{-140.0}$	$0.75^{+0.06}_{-0.06}$	$0.31^{+0.43}_{-0.28}$	$0.74^{+0.17}_{-0.59}$	$0.54^{+0.35}_{-0.59}$	−0.00	−0.47	−0.09
GW200224_222234	$90.3^{+6.4}_{-6.3}$	$84.4^{+23.2}_{-20.3}$	$88.6^{+15.5}_{-15.2}$	$119.4^{+142.6}_{-34.3}$	$0.73^{+0.06}_{-0.07}$	$0.61^{+0.27}_{-0.49}$	$0.60^{+0.23}_{-0.42}$	$0.64^{+0.27}_{-0.59}$	0.20	0.95	−0.11
GW200311_115853	$72.1^{+5.4}_{-4.7}$	$68.5^{+23.6}_{-13.5}$	$72.2^{+28.6}_{-16.3}$	$213.2^{+167.8}_{-141.5}$	$0.68^{+0.07}_{-0.08}$	$0.30^{+0.44}_{-0.28}$	$0.58^{+0.30}_{-0.47}$	$0.56^{+0.32}_{-0.54}$	0.02	−1.16	−0.15

LVK, 2112.06861

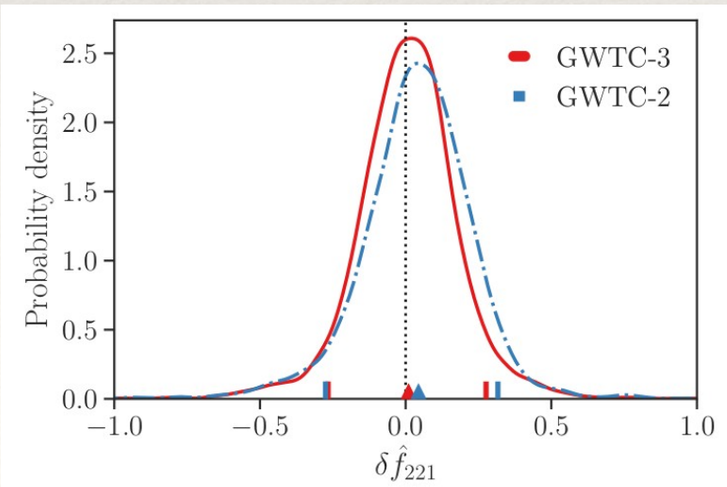

Spectroscopy of GW150914

Isi et al., PRL 2019

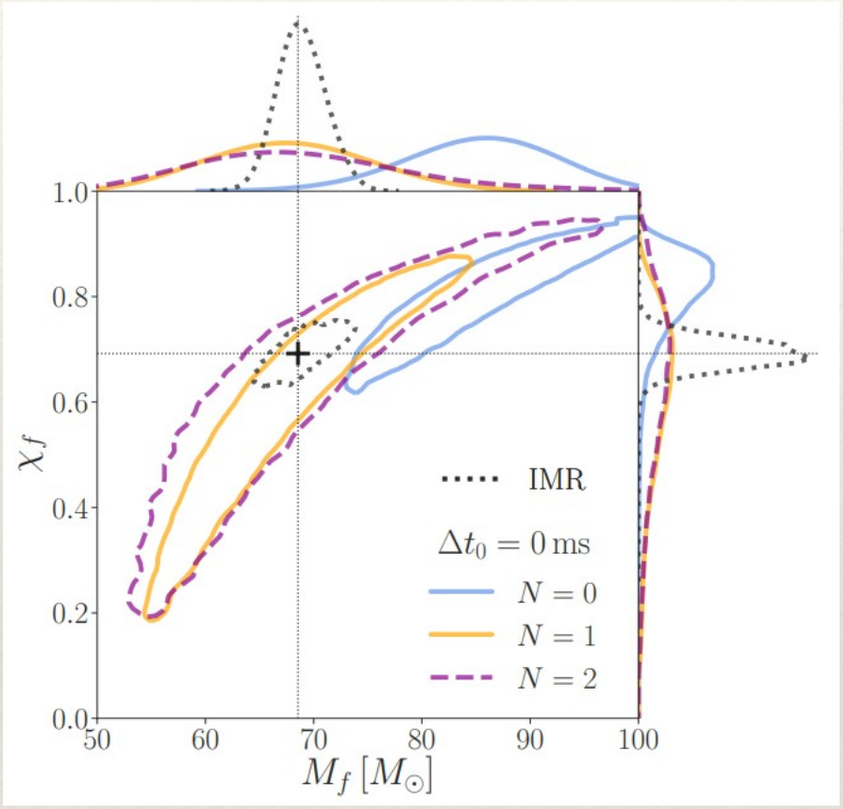

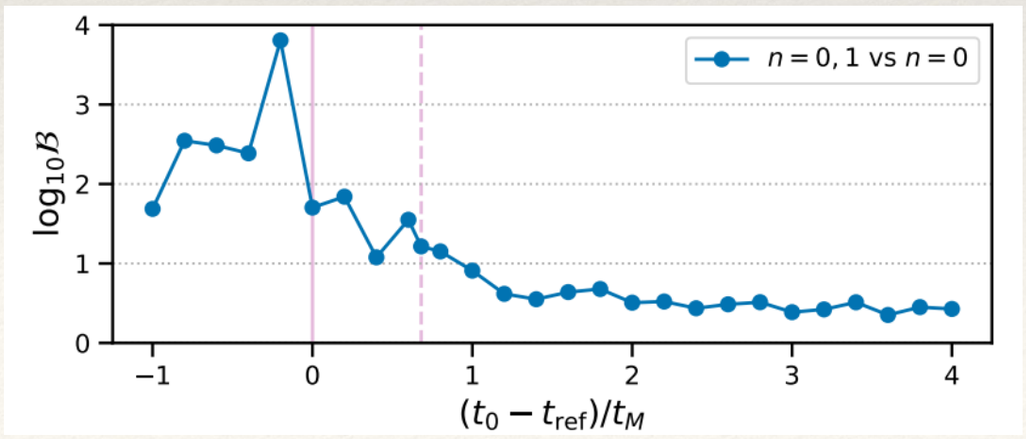

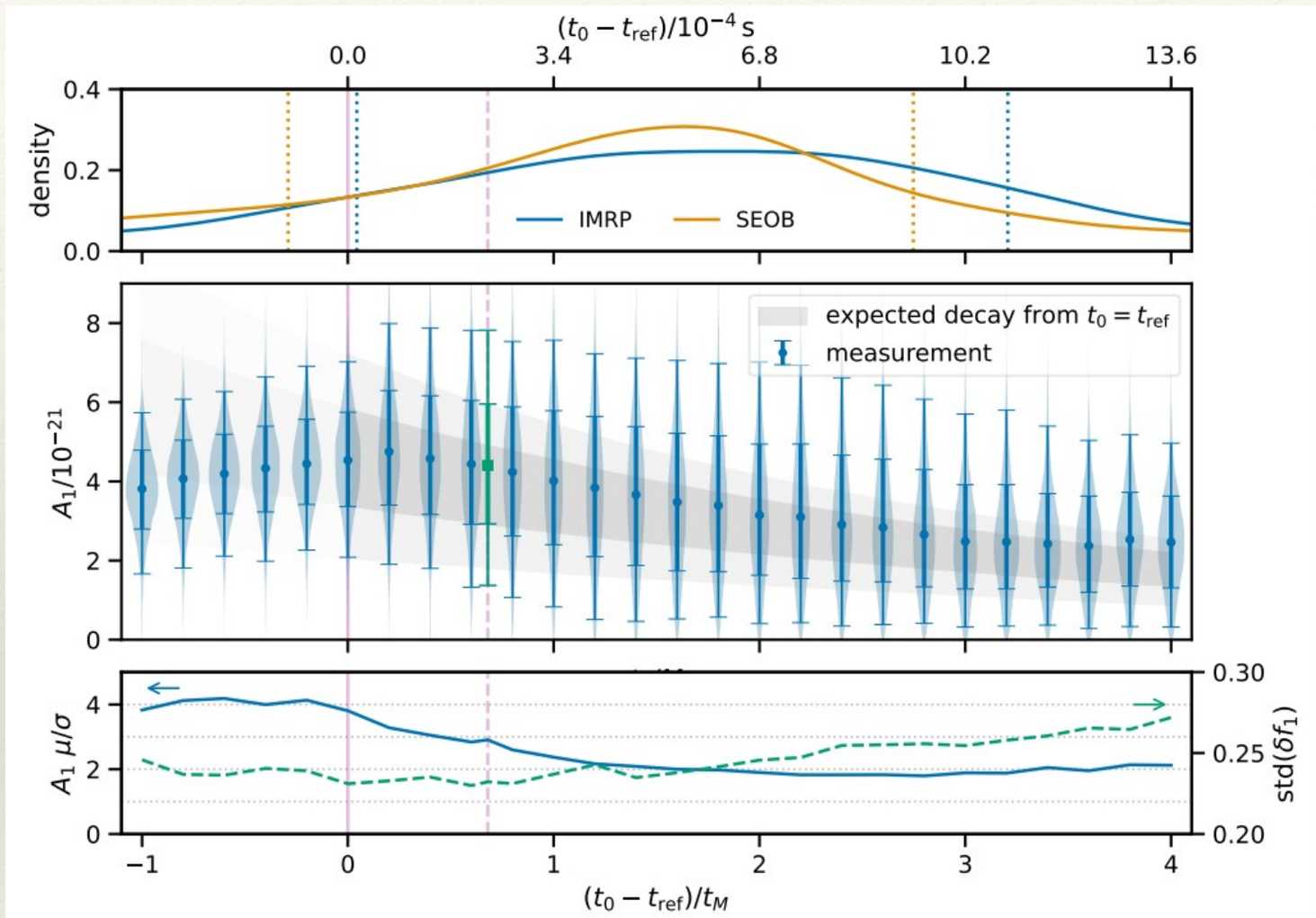

Isi et al., 2202.02941

- Fit from the peak, based on the results of Giesler et al., PRX 2019
- Suggest to add higher modes as long as their posterior favour non-zero values

Spectroscopy of GW150914

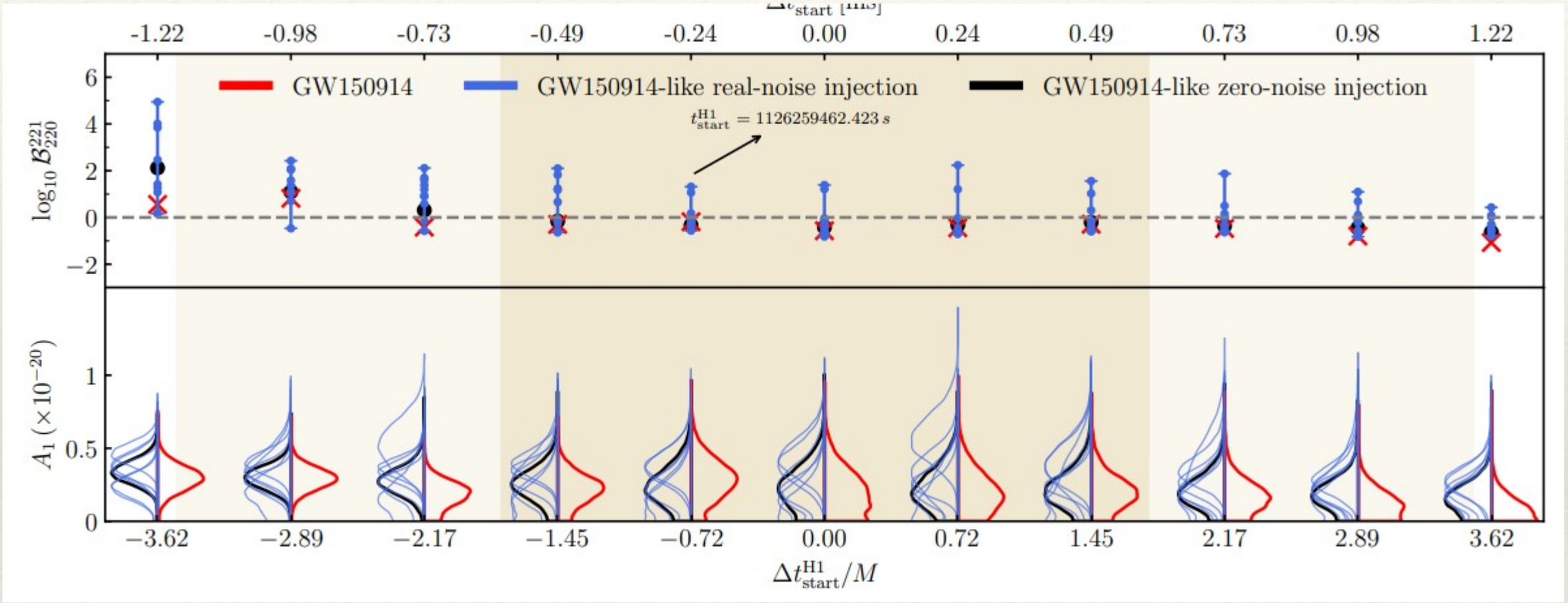

Carullo et al., 2310.20625

- Disagreement whether there is support for an overtone or not.

Spectroscopy of GW150914

- Spectroscopy is typically performed in time-domain because the signal is too short and we cannot properly window it before doing Fourier transform
- An alternative is to extend the signal before the ringdown using an agnostic model, e.g. wavelets:

$$h(t) = h^{\rm IM}(t) + h^{\rm R}(t)$$

$$h^{\rm IM}(t) = h^{\rm IM}_{+}(t) - i h^{\rm IM}_{\times}(t) = \sum_{w=1}^{W} \mathcal{A}_w \exp\left[-2\pi i \nu_w (t-\eta_w) - (\frac{t-\eta_w}{\tau_w})^2 + i\varphi_w \right]$$

$$h^{\rm R}(t) = h^{\rm R}_{+}(t) - i h^{\rm R}_{\times}(t) = \sum_{\ell mn} A_{\ell mn} e^{-i[\omega_{\ell mn}(t-t_0)-\phi_{\ell mn}]}, \quad t \geq t_0$$

Finch, PRD 2021

- Allows to marginalise over sky location and starting time instead of fixing them.

Spectroscopy of GW150914

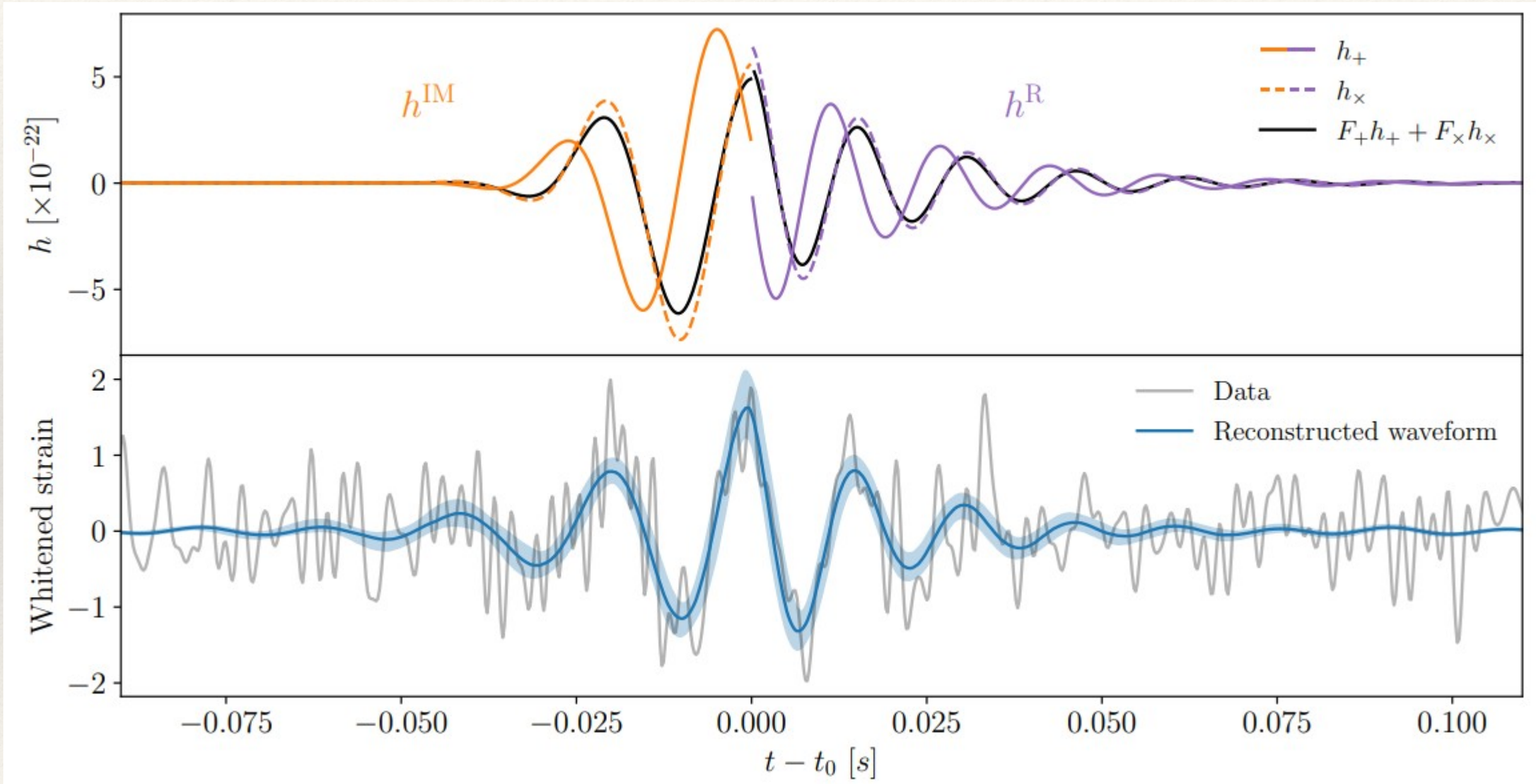

Finch, PRD 2021

Spectroscopy of GW150914

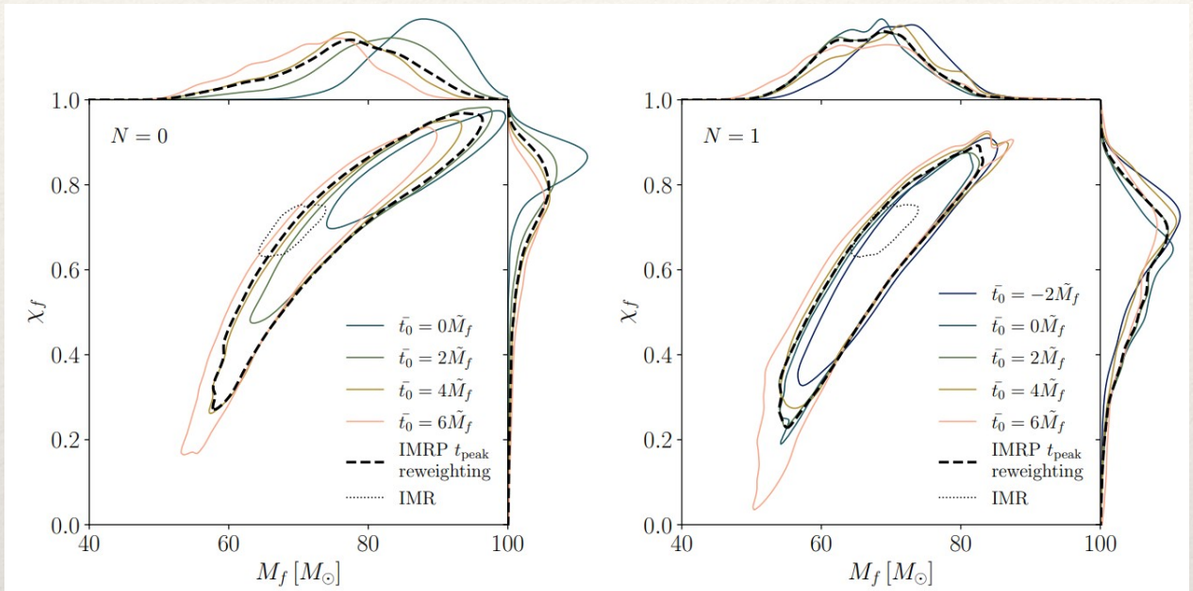

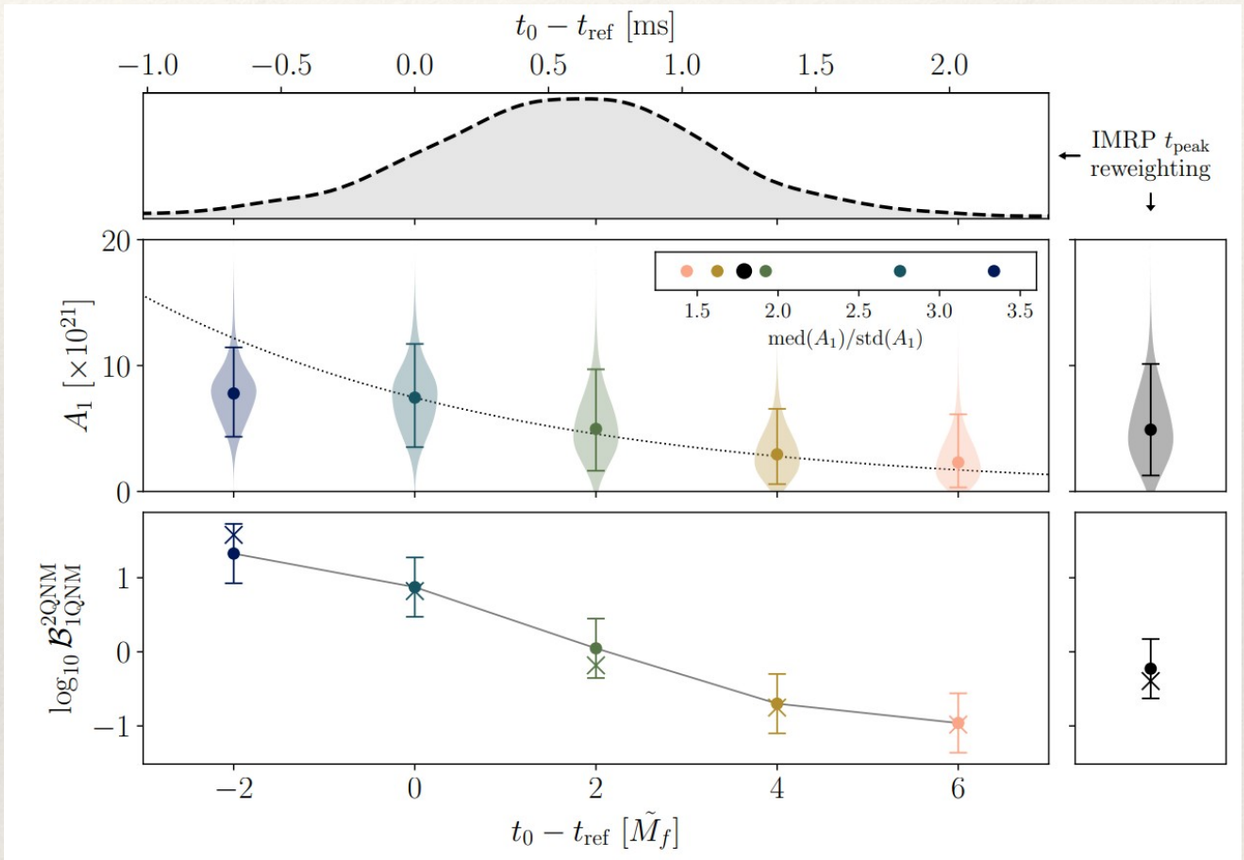

Finch, PRD 2021

- Also finds evidence for an overtone, although less strong than Isi et al..
- Similar conclusio in Wang et al., 2310.19645
- Also claims of detection of beyond dominant QNM in GW190521, possibly (2,1,0), but not sure.

Source reconstruction

BayesWave

- The *BayesWave* pipeline uses a Bayesian non-parametric approach to reconstruct noise and signal components from the data.
- The smooth noise PSD component is modelled using a cubic spline.
- Lines in the instrumental noise are modelled using Lorentzian functions.

$$p(x; b, m) = \frac{1}{\pi} \frac{b}{(x-m)^2 + b^2}$$

- The remaining components of the data are modelled using *wavelets*, which resolve time series at particular times and frequencies. *BayesWave* uses the Morley-Gabor basis.
- There is a coherent wavelet component for sources and incoherent components to represent glitches.
- Also used to look for additional features in data, e.g. echoes

BayesWave

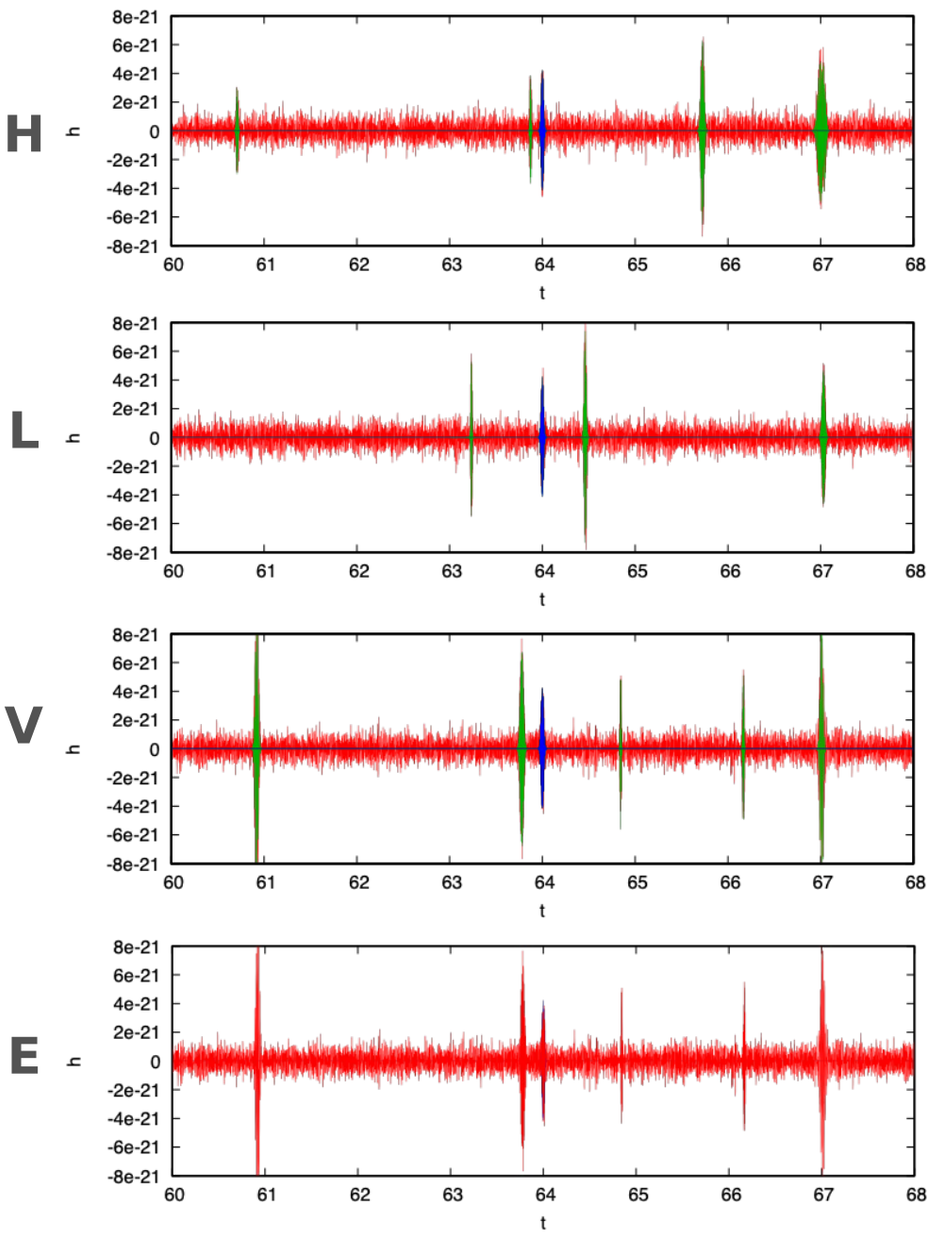

Independent

Coherent

$$d^H = n^H + \sum_i^{N_G^H} \psi(\vec{\gamma}_i^H) + h^H(N_{\rm GW}^{\oplus}, \vec{\gamma}^{\oplus}, \vec{\lambda}\,)$$

$$d^L = n^L + \sum_i^{N_G^L} \psi(\vec{\gamma}_i^L) + h^L(N_{\rm GW}^{\oplus}, \vec{\gamma}^{\oplus}, \vec{\lambda}\,)$$

$$d^V = n^V + \sum_i^{N_G^V} \psi(\vec{\gamma}_i^V) + h^V(N_{\rm GW}^{\oplus}, \vec{\gamma}^{\oplus}, \vec{\lambda}\,)$$

$$h^{\rm IFO} = \mathcal{R}^{IFO}(\vec{\lambda}) * \sum_i^{N_{\rm GW}^{\oplus}} \psi(\vec{\gamma}_i^{\oplus})$$

Extrinsic

Intrinsic

$\{\vec{\Omega}, \delta\phi_{\oplus}, \delta t_{\oplus}, \delta\mathcal{A}, \psi, e\}$

sky location, orientation, etc.

$\{t_0, f_0, \mathcal{A}, \text{etc.}\}$

morphological params.

BayesWave

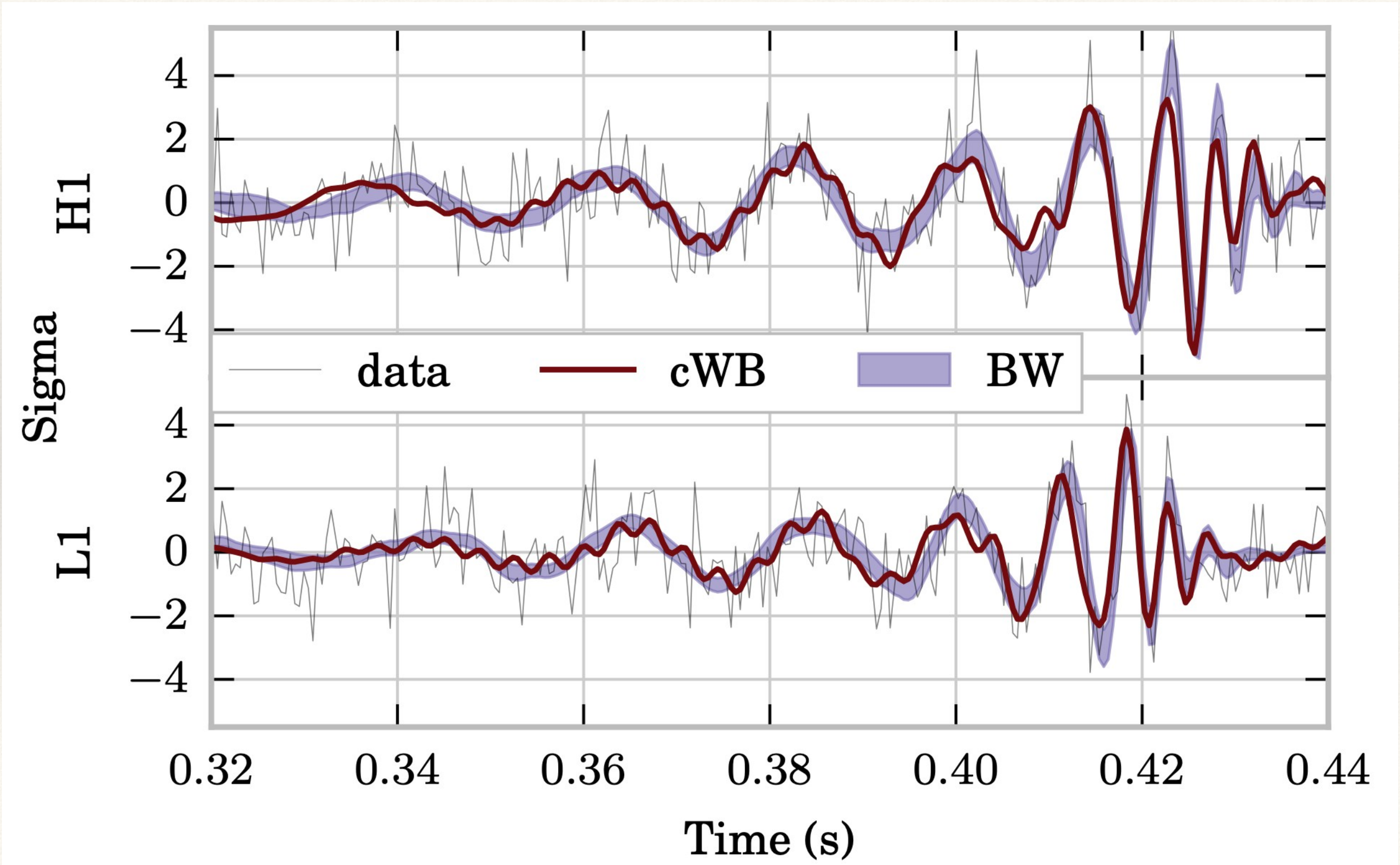

Population Inference

Population Inference

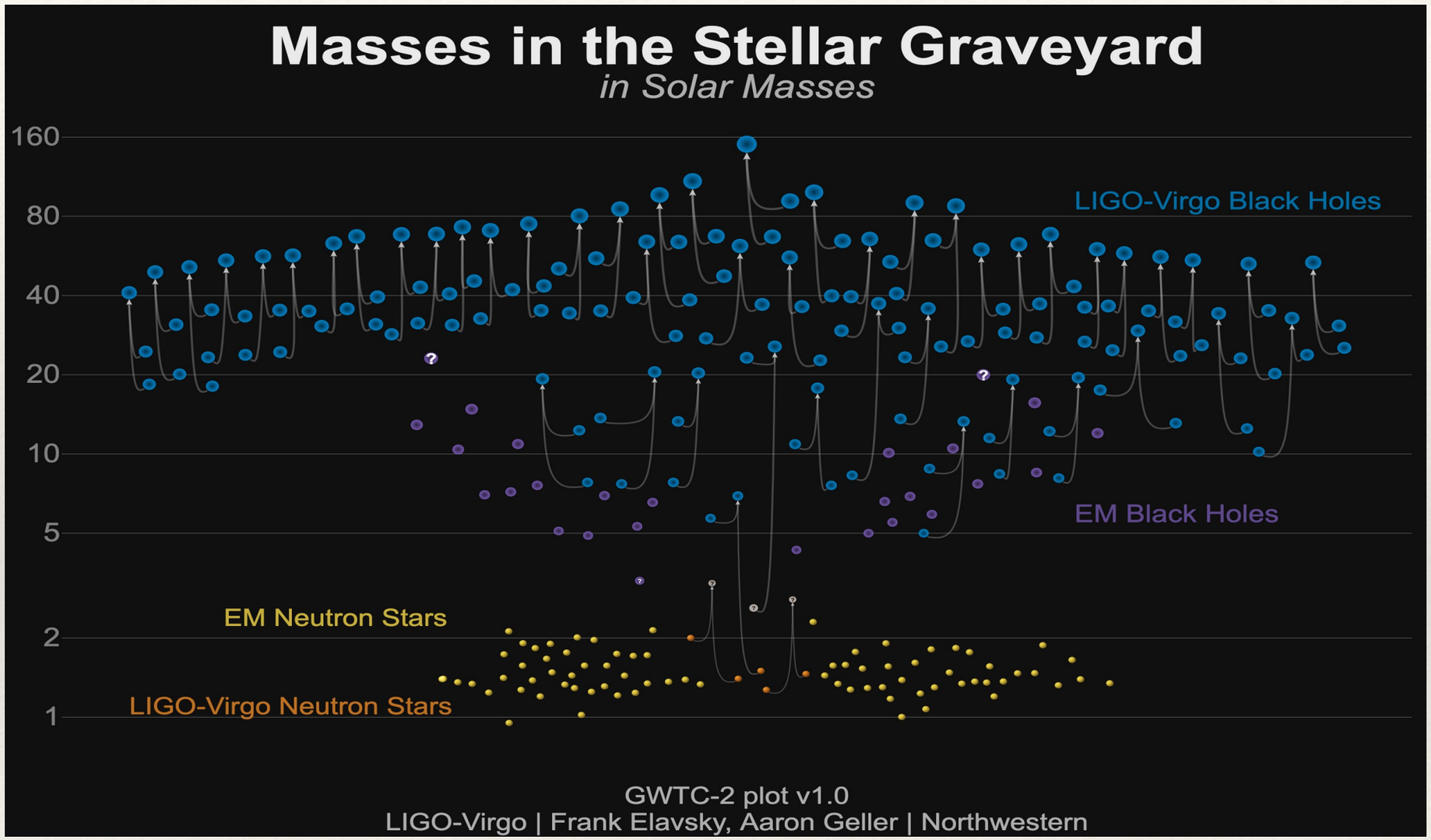

- **Goal:** Understand which astrophysical/cosmological model describes better GW observations as a whole

Formation channels for stellar-mass black hole binaries (sBHBs)

- **Isolation:**
  - Mass gap between $\sim 60 - 120 M_{\odot}$
  - Aligned spins
  - Quasi-circular

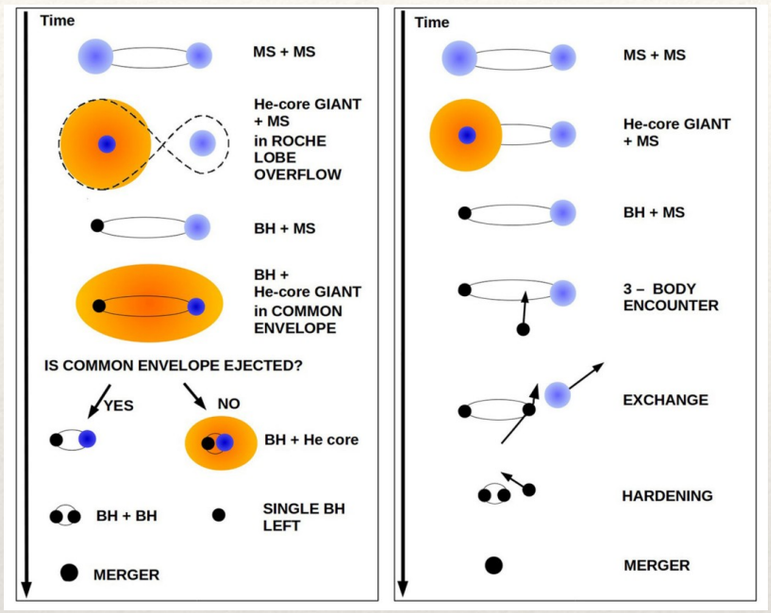

Mapelli, Frontiers in Astronomy and Space Sciences 2020

- **Dynamical:**
  - Dense stellar clusters
  - Second generation mergers can be more massive
  - Isotropic spins
  - Larger eccentricities

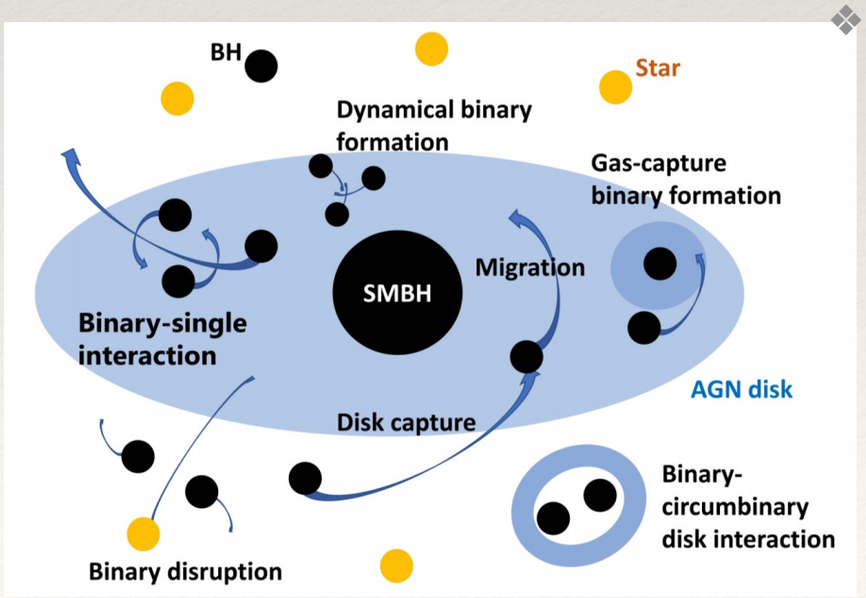

Tagawa et al. APJ 2020

- **AGN:**
  - Potentially more massive (second generation)
  - Spins tend to align with central BH
  - Larger eccentricities

Astrophysical inference

- Assume a form for $p_{\rm pop}(m_1, m_2, \chi_1, \chi_2, z|\lambda)$
- Can be:
  - astrophysical
  - parametric
  - non-parametric
- Obtain $p_{\rm pop}(\lambda|\{d\})$ accounting for selection effects and measurement uncertainty performing a hierarchical Bayesian analysis

Astrophysical model

- Results on GWTC-2 from Wong et al., PRD 2021

$$p_{\rm pop}(m_1, m_2, z|\alpha, r_v, f) = f p_{\rm iso}(m_1, m_2, z|\alpha) + (1-f) p_{\rm dyn}(m_1, m_2, z|r_v)$$

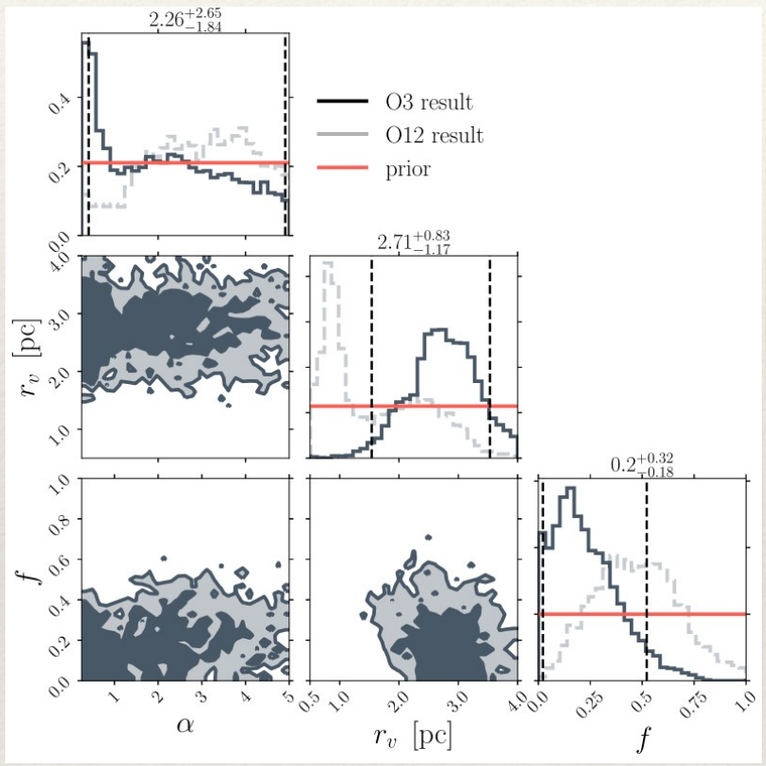

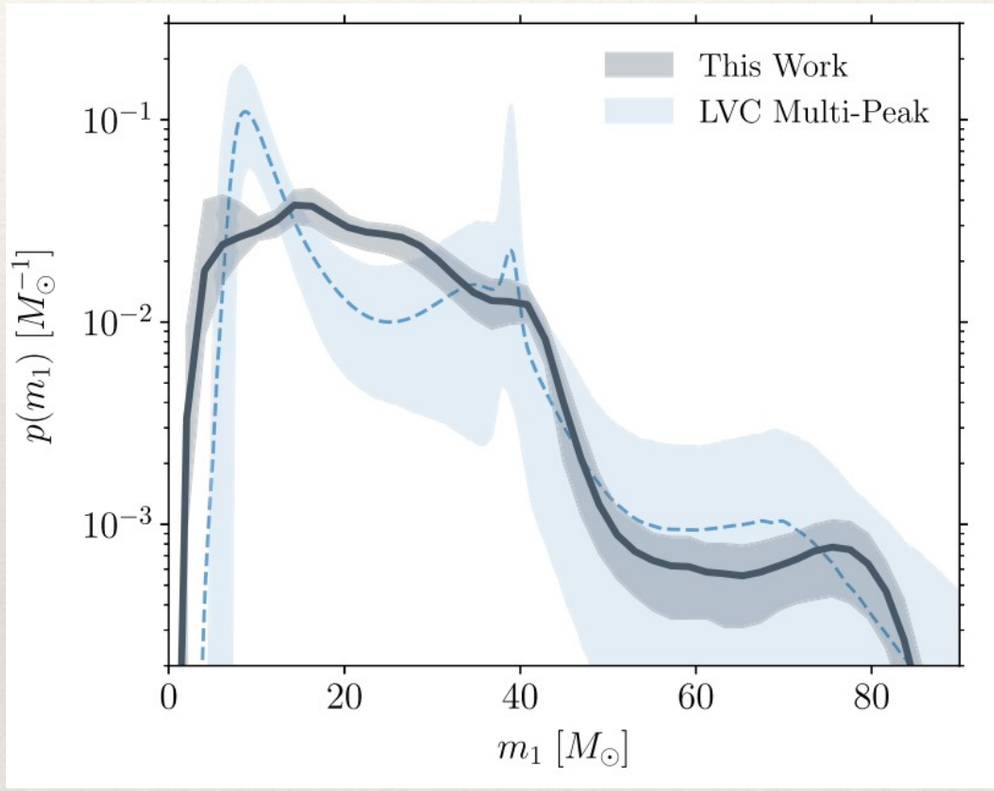

- See Zevin et al., APJ 2021 for more formation channels et Mould et al., PRD 2022 for results on GWTC-3
- **Pros:**
  - Gives direct information on astrophysical processes
- **Cons:**
  - Huge uncertainty on astro models. We might not include all channels (see Cheng et al., 2307.03129, Raikman et al., 2310.10736)
  - Requires some way to evaluate pdf from samples and to interpolate (see Toubiana et al., PRD 2021 for systematic errors)

Parametric model

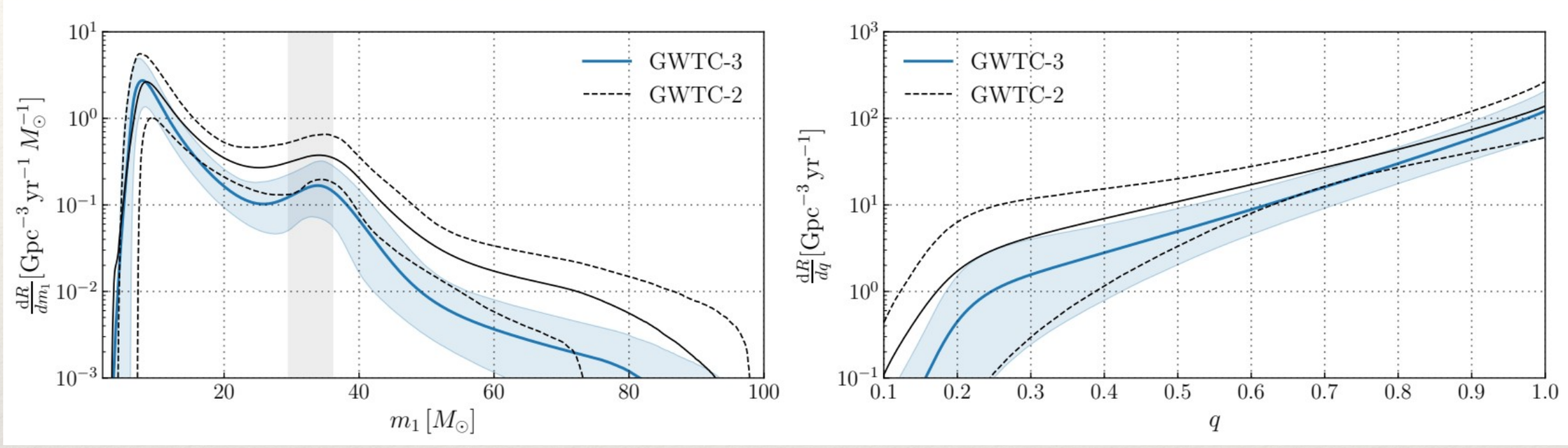

LVK, PRX 2021

$$p_{\rm pop}(m_1|\Lambda) = [\lambda \mathrm{G}(m_1, \mu, \sigma) + (1-\lambda)\mathrm{PL}(m_1, m_{min}, m_{max}, \alpha)]S(m_1, m_{min}, \delta_m)$$

$$p_{\rm pop}(q|m_1, \Lambda) \propto q^\beta S(qm_1, m_{min}, \delta_m)$$

$$R(z) = R_0(1+z)^\kappa$$

- GWTC-3 shows evidence for a peak at $\sim 35 M_\odot$, a bit low for the pair-instability gap
- Some evidence for for rate evolution, with the rate higher in the past.

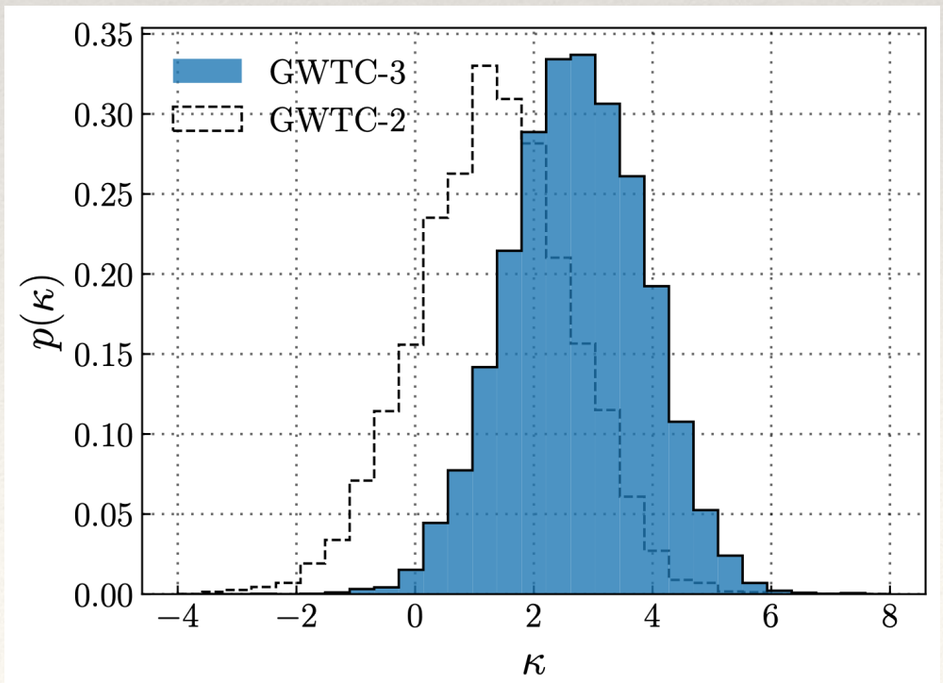

Parametric model

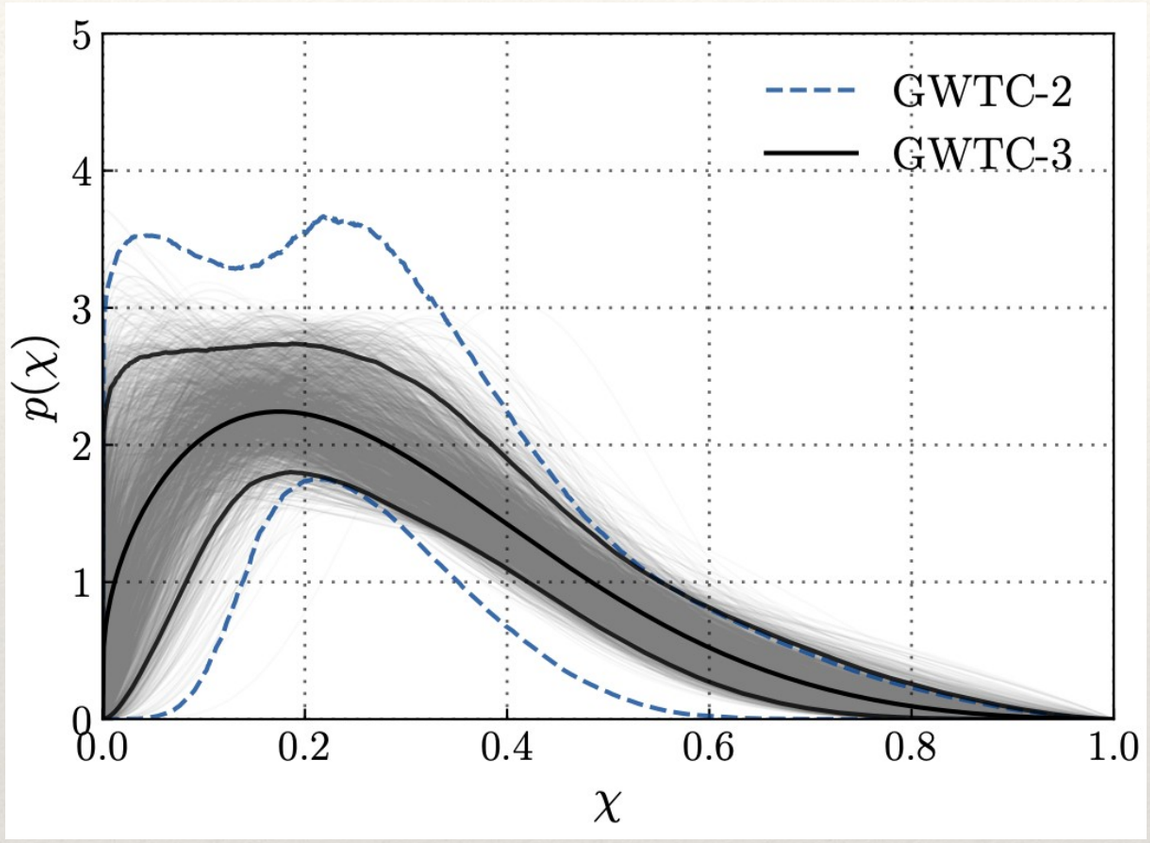

$$p_{\rm pop}(\chi_i|\alpha,\beta) = \frac{\chi_i^{\alpha-1}(1-\chi_1)(\beta-1)}{B(\alpha,\beta)}$$

$$p_{\rm pop}(\cos t_1, \cos t_2|\zeta,\sigma_t) = \frac{1-\zeta}{4} + \frac{2\zeta}{\pi\sigma_t^2 {\rm erf}(\sqrt{2}/\sigma_t)^2} \exp\left[-\frac{(1-\cos t_1)^2+(1-\cos t_2)^2}{\sigma_t^2}\right]$$

LVK, PRX 2021

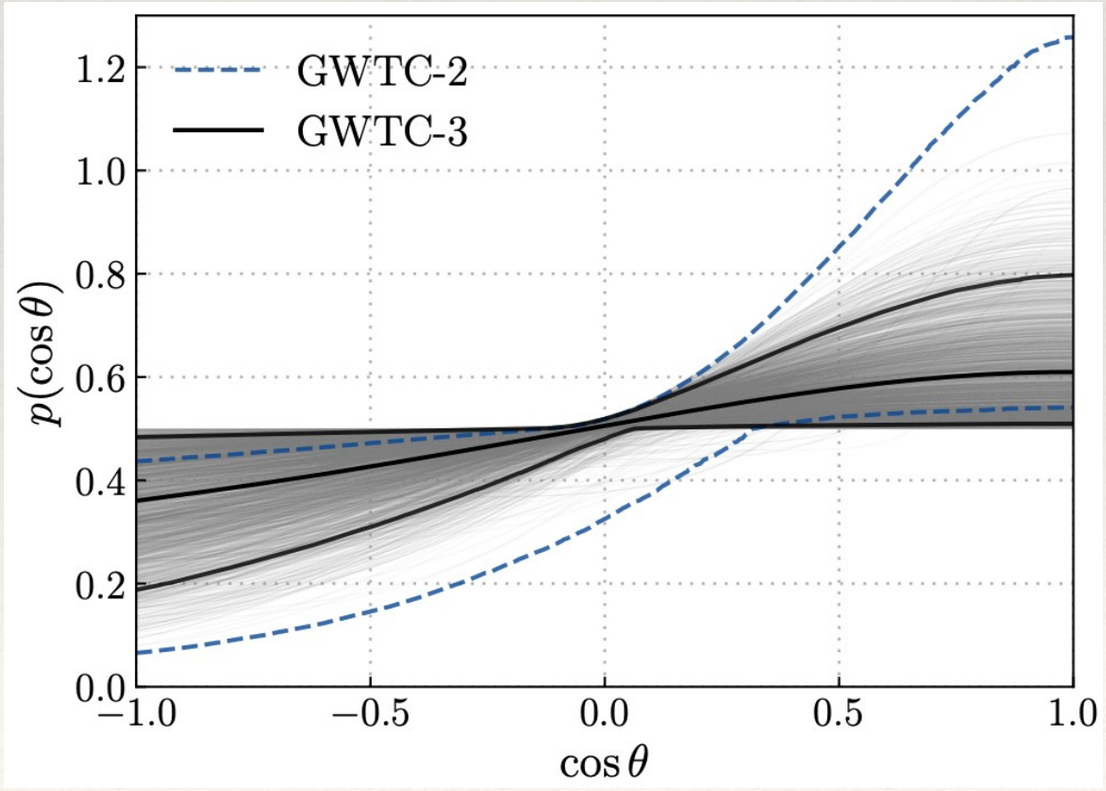

- Moderate spins are favoured
- Small preference for aligned spins

Parametric model, multi-dimensional

- Probe correlations between parameters by fitting joint distributions, or allowing model parameters to depend on other parameters. In the analysis of GWTC-3, the LVK explored the variation of the spin distribution with mass ratio.

$$p_{\rm pop}(\chi_{\rm eff}|q) \propto \exp\left[-\frac{(\chi_{\rm eff}-\mu(q))}{2\sigma(q)^2}\right]$$

$$\mu(q) = \mu_0 + \alpha(q-1)$$

$$\log_{10}\sigma(q) = \log_{10}(\sigma_0) + \beta(q-1)$$

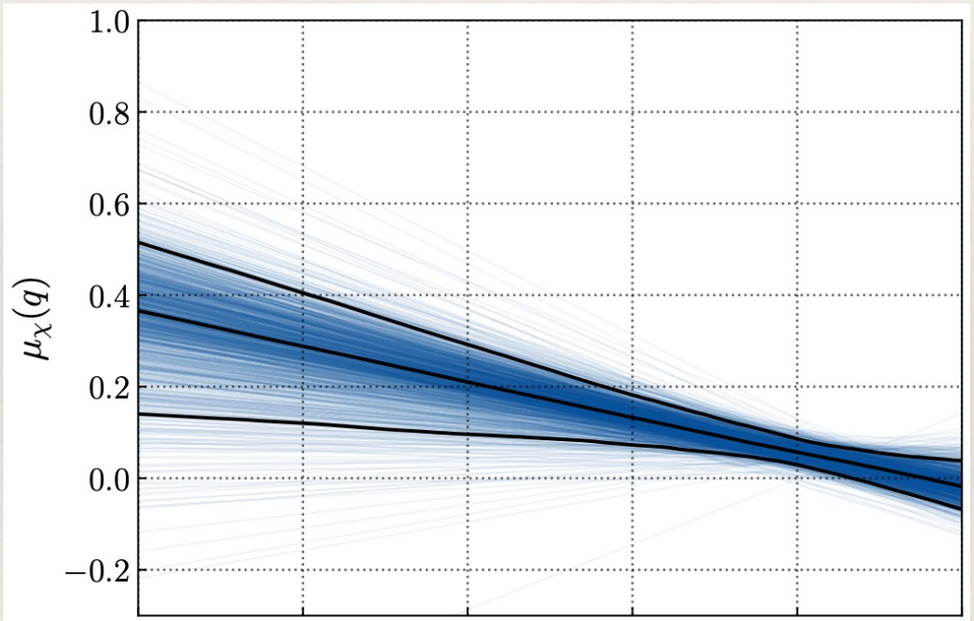

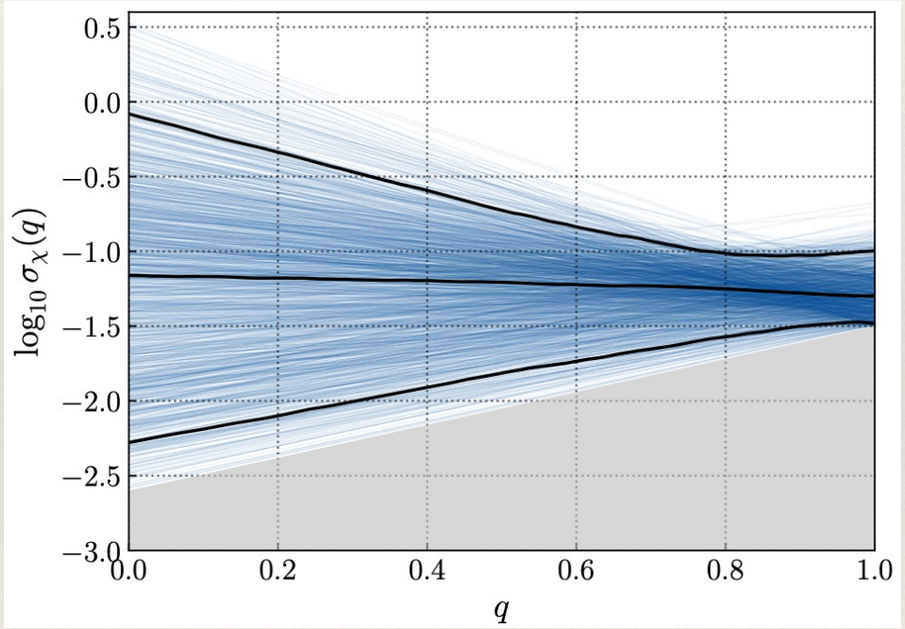

- Also hints of correlation between effetctive spin and redshift (Biscoveanu et al., APJL 2022), mass and redshift (Fishbach et al., APJ 2021), mass and spins (Hoy et al., APJ 2022, non-parametric: Godfrey et al., 2304.01288, Rinaldi et al., 2310.03074)
- **Pros:**
  - Analytic pdfs, easy to evaluate
  - Some astrophysical meaning
- **Cons:**
  - Little flexibility
  - Not so much astrophysical meaning

Non-parametric model

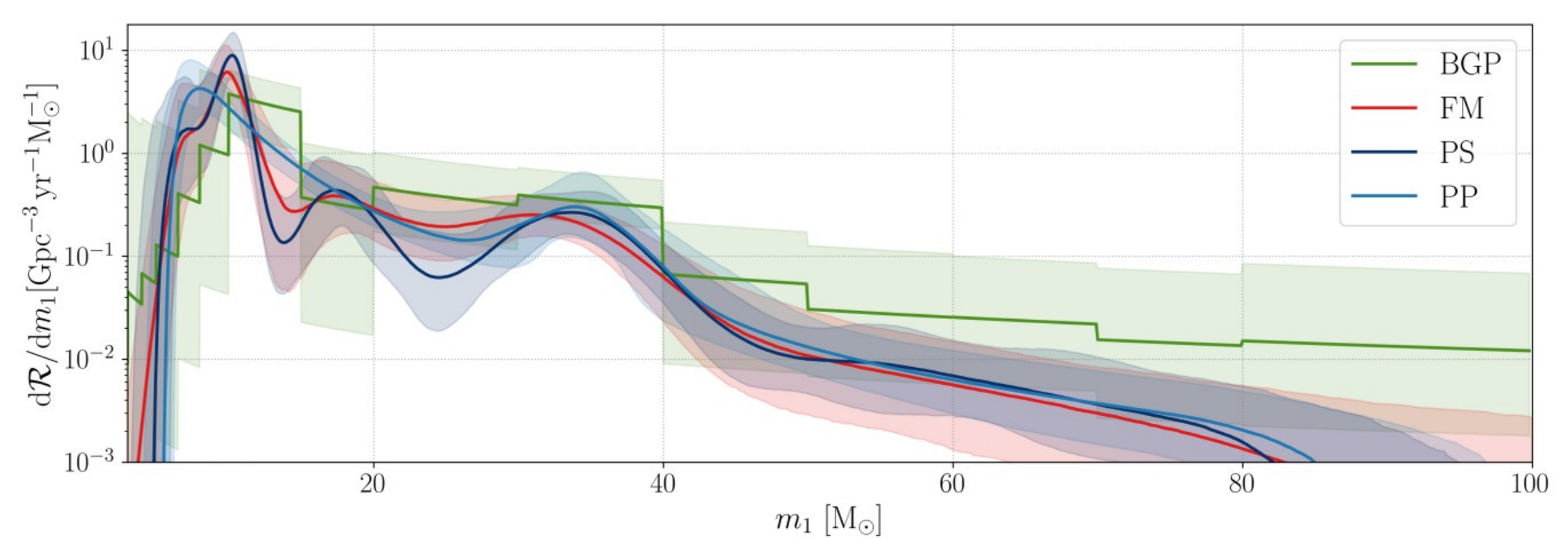

LVK, PRX 2021

- BGP: Binned Gaussian process
- FM: Flexible mixture, total pdf is the sum of elementary functions, here Gaussian for the primary mass, the spins and power-laws for mass ratio
- PS: power-law spline, pdf is power-law times a spline which value at fixed knots is inferred, presence of peak is not imposed

Non-parametric model

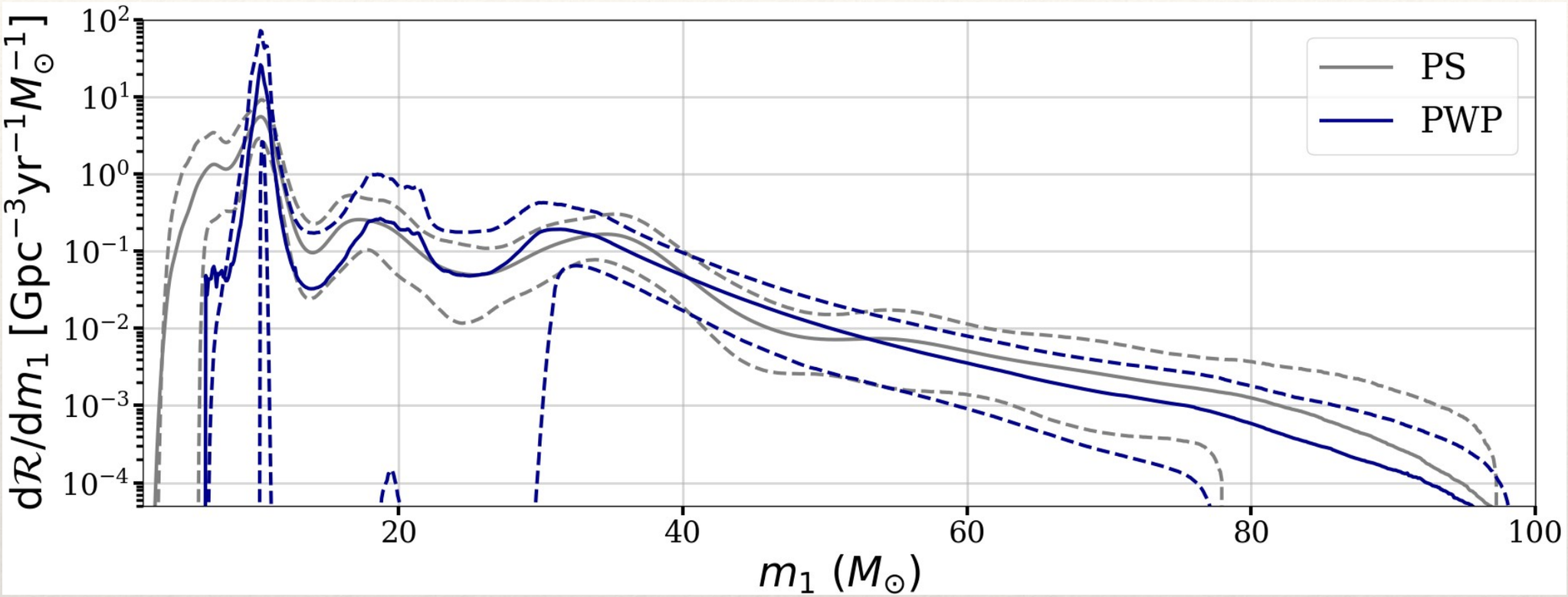

Toubiana et al., MNRAS 2023

- Model the pdf as a piece-wise power-law, vary the position and the number of knots using RJMCMC.
- Performing (simplified) posterior predictive checks we find a 5% probability of peak at $\sim 20 M_\odot$ to be spurious.

Non-parametric model

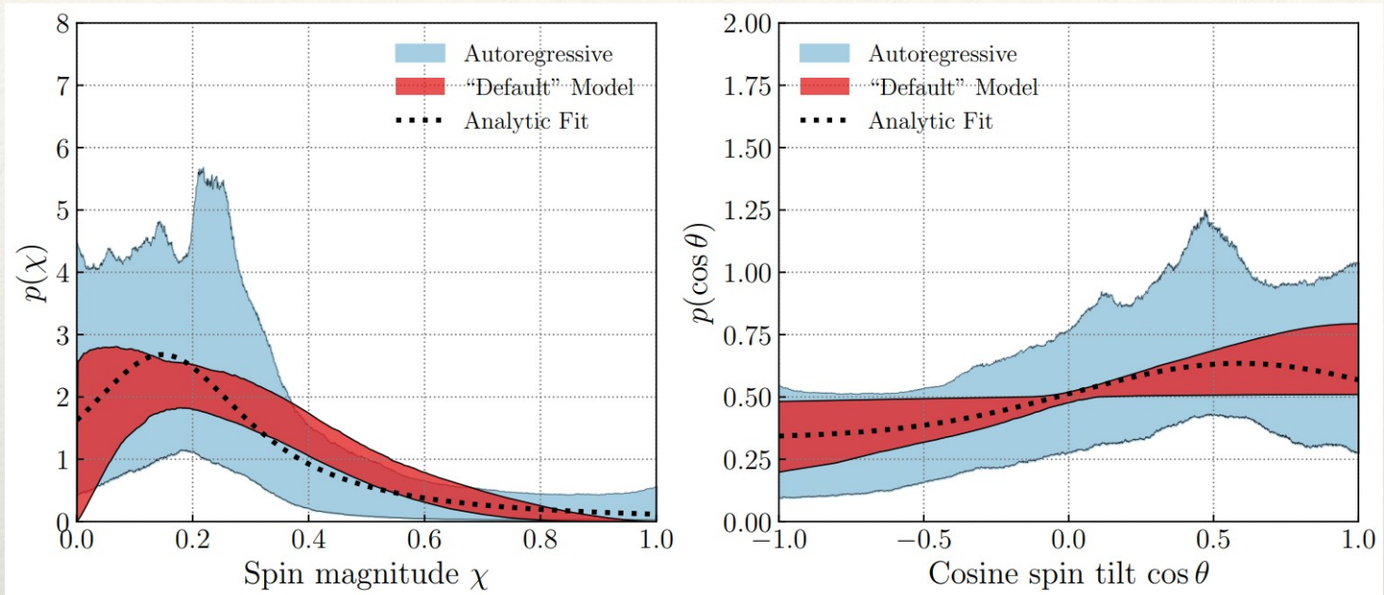

Callister et al., 2302.07289

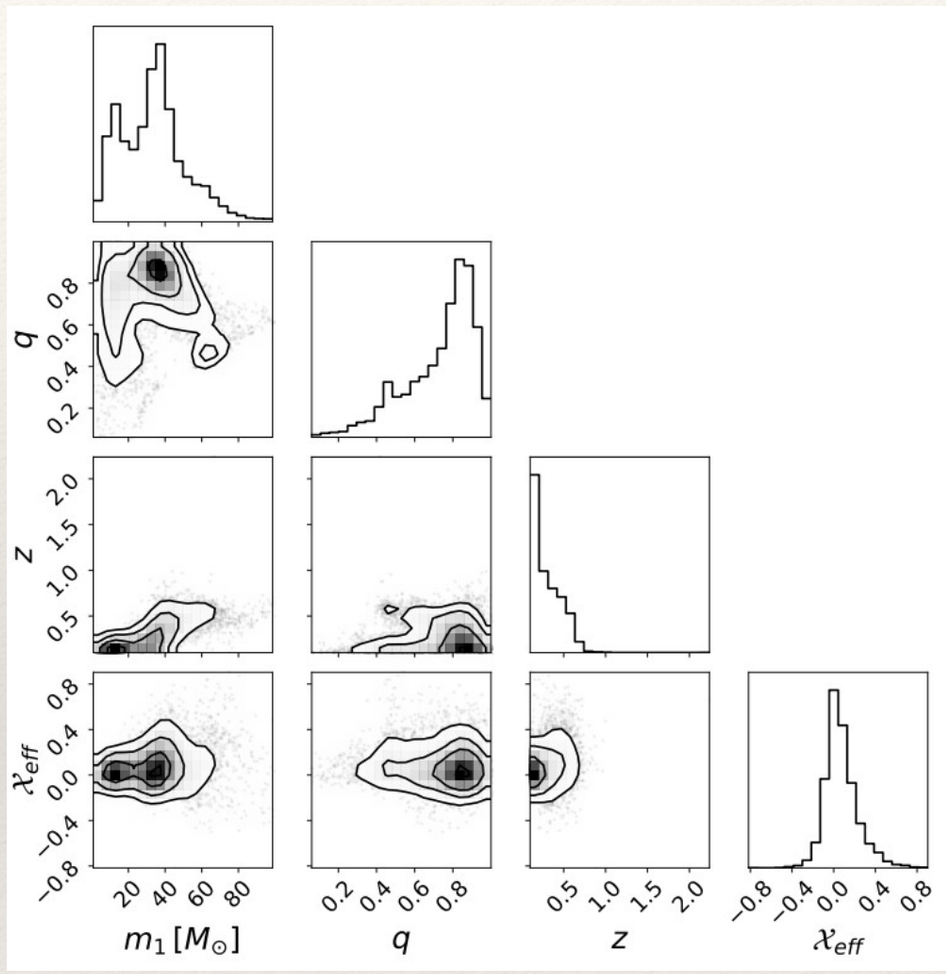

Ruhe et al., 2211.09008v3

- Note: here selection effects are not included

- **Pros:**
  - Very flexible
  - Requires less a prior knowledge
- **Cons:**
  - Parameters have no astrophysical meaning
  - Complexity is a priori arbitrary (might be alleviated using RJMCMC)

Rate estimation: GWTC-3

- .

	$m_1 \in [5,20]M_\odot$ $m_2 \in [5,20]M_\odot$	$m_1 \in [20,50]M_\odot$ $m_2 \in [5,50]M_\odot$	$m_1 \in [50,100]M_\odot$ $m_2 \in [5,100]M_\odot$	All BBH
PP	$23.4^{+12.9}_{-8.6}$	$4.5^{+1.8}_{-1.3}$	$0.2^{+0.1}_{-0.1}$	$28.1^{+14.8}_{-10.0}$
BGP	$20.0^{+10.0}_{-8.0}$	$6.4^{+3.0}_{-2.1}$	$0.74^{+1.2}_{-0.46}$	$33.0^{+16.0}_{-10.0}$
FM	$21.1^{+10.7}_{-8.3}$	$4.1^{+2.0}_{-1.4}$	$0.2^{+0.3}_{-0.1}$	$26.0^{+11.5}_{-8.7}$
PS	$27^{+12}_{-9.4}$	$3.6^{+1.5}_{-1.1}$	$0.2^{+0.18}_{-0.1}$	$32^{+14}_{-9.6}$
MERGED	$12.8 - 40$	$0.098 - 6.3$	$2.5 - 0.5$	$17.3 - 45$

	BNS $m_1 \in [1,2.5]M_\odot$ $m_2 \in [1,2.5]M_\odot$	NSBH $m_1 \in [2.5,50]M_\odot$ $m_2 \in [1,2.5]M_\odot$	BBH $m_1 \in [2.5,100]M_\odot$ $m_2 \in [2.5,100]M_\odot$	NS-Gap $m_1 \in [2.5,5]M_\odot$ $m_2 \in [1,2.5]M_\odot$	BBH-gap $m_1 \in [2.5,100]M_\odot$ $m_2 \in [2.5,5]M_\odot$	Full $m_1 \in [1,100]M_\odot$ $m_2 \in [1,100]M_\odot$
PDB (pair)	960^{+1700}_{-700}	59^{+81}_{-38}	25^{+10}_{-7}	41^{+69}_{-30}	$9.3^{+19.0}_{-7.6}$	1100^{+1700}_{-750}
PDB (ind)	250^{+640}_{-200}	170^{+150}_{-89}	22^{+9}_{-6}	29^{+55}_{-23}	10^{+15}_{-8}	470^{+830}_{-300}
MS	470^{+1400}_{-410}	57^{+120}_{-42}	42^{+88}_{-20}	$3.7^{+20}_{-3.4}$	$0.17^{+56}_{-0.16}$	650^{+1600}_{-460}
BGP	99^{+260}_{-86}	32^{+62}_{-25}	33^{+16}_{-10}	$2.1^{+33}_{-2.1}$	$5.1^{+12}_{-4.0}$	180^{+260}_{-110}
MERGED	$13 - 1900$	$7.4 - 320$	$16 - 130$	$0.029 - 84$	$0.01 - 56$	$71 - 2200$

LVK, PRX 2021

Fitting all the mass spctrum

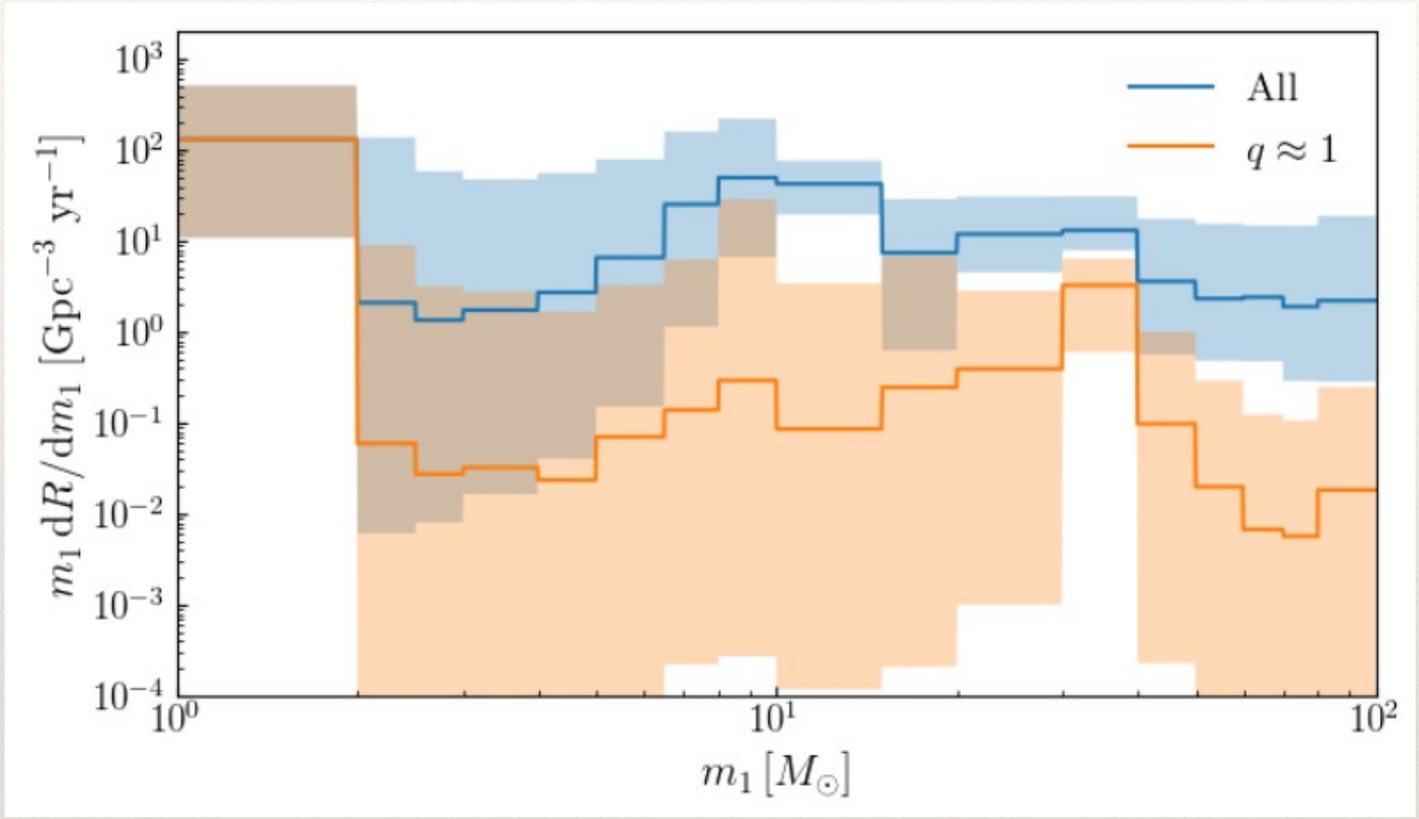

LVK, PRX 2021

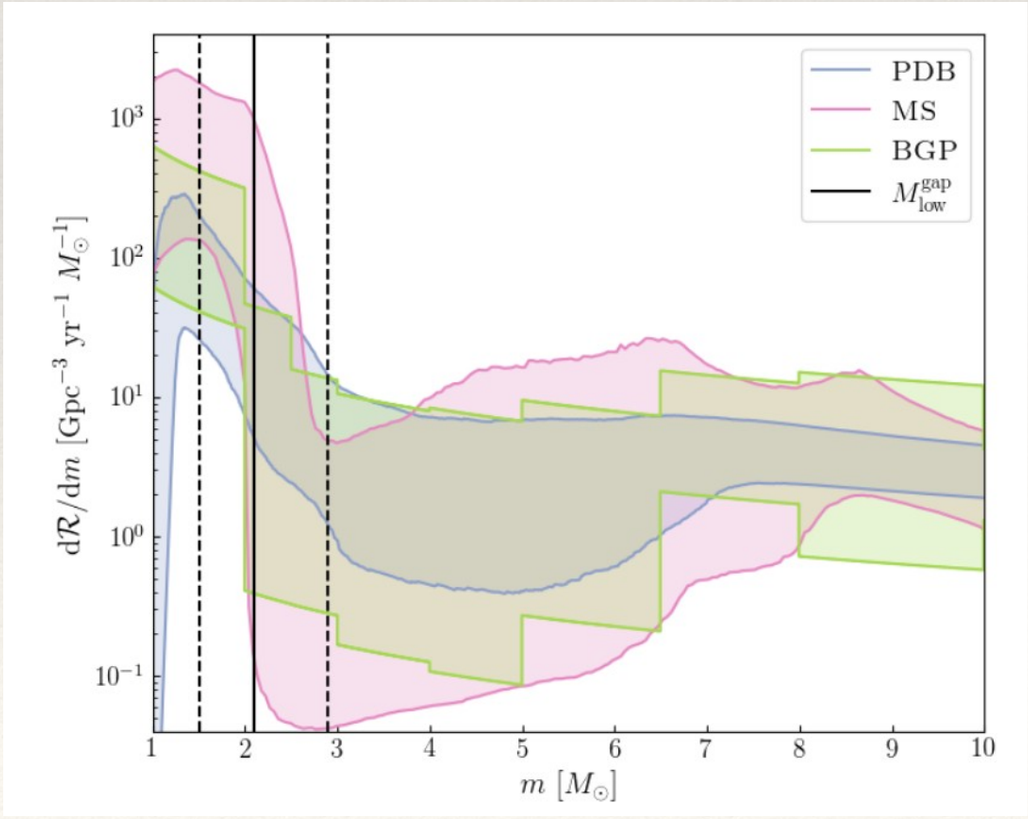

Future challenges

- Computational cost scales (naively) with the number of events:

$$\prod_i \int p(d_i|\theta)p(\theta|\lambda)\mathrm{d}\theta = \prod_i \frac{p(d_i|\lambda)}{N_s} \sum_{\theta_j \sim p(\theta|d_i)} \frac{p(\theta_j|\lambda)}{\pi_{\mathrm{PE}}(\theta_j)}$$

- Selection function computation might become inaccurate (see Essick et al., 2204.00461)

$$p_s(\lambda) = \frac{1}{N_{\mathrm{inj}}} \sum_{\theta \sim p_{\mathrm{inj}},\ \mathrm{det}} \frac{p(\theta|\lambda)}{p_{\mathrm{inj}}(\theta)}$$

- "Systematics" in the population model might significantly bias the results

- Make the link with EM observations (see Fisbach et al., APJL 2022, Belczynski et al., 2111.0940, Liotine et al., APJ 2023)

Cosmological Inference

Cosmological inference

- Several possibilities to infer cosmology with Gws.
- Bright sirens:
  - If EM counterpart, combine with redshift measurement.
- Dark sirens
  - Correlate observations with galaxy catalogues to get a statistical measurement of the redshift of the source
  - Include the impact of cosmology on the observed distribution of events
    $m_{\rm det} = (1+z) m_{\rm source}$

Cosmological inference

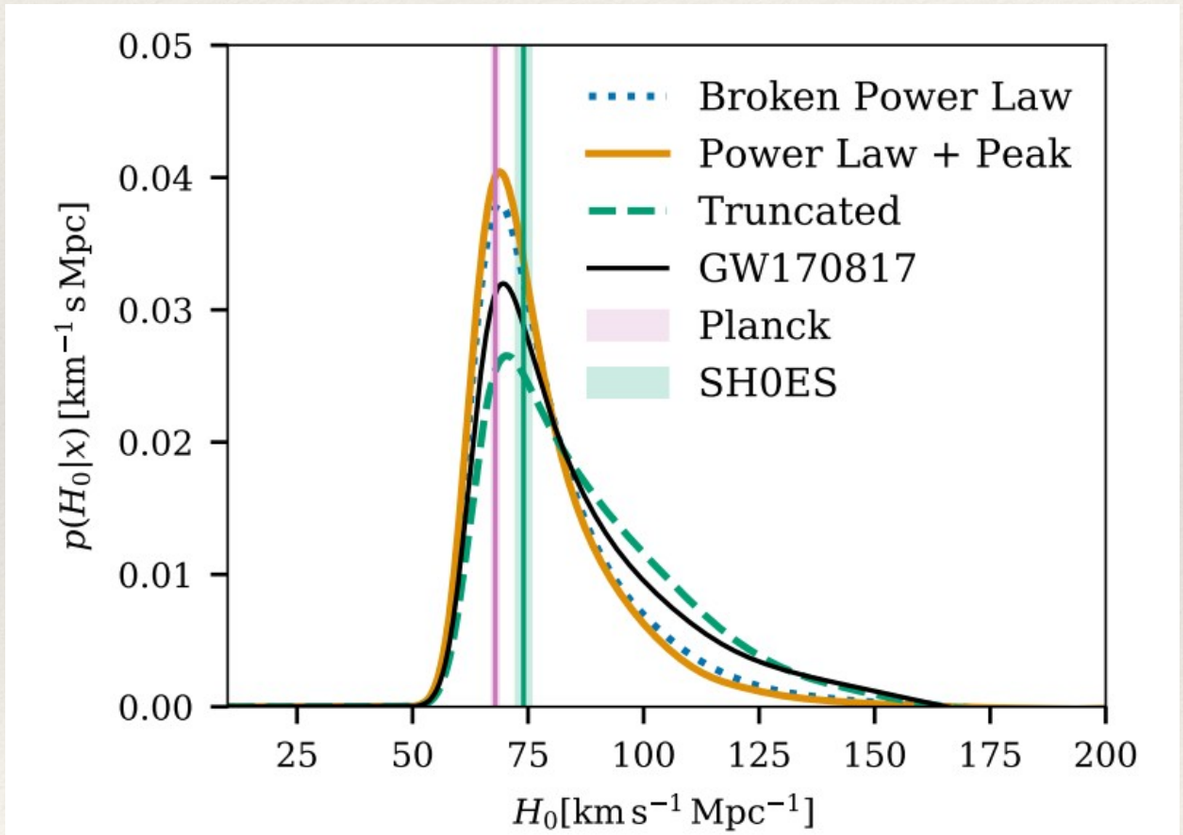

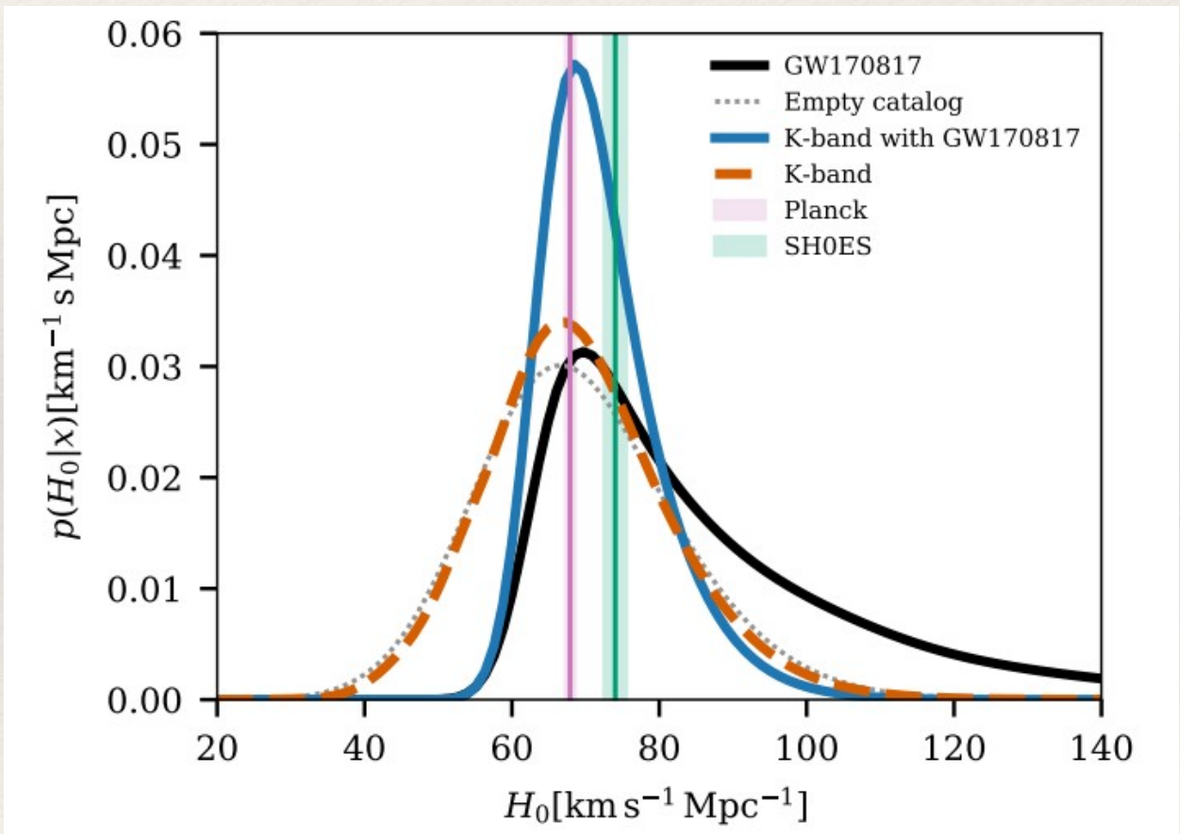

LVK, APJ 2023

Rapid localisation

Bayestar

- Bayesian techniques are also used to obtain rapid sky localisation of GW transients to send triggers to astronomers for EM follow-up.

- **Bayestar** employs the **autocorrelation likelihood** (likelihood evaluated at MLE parameter values)

$$\exp\left[-\frac{1}{2}\sum_i {\rho_i}^2 + \sum_i \rho_i \Re\left\{e^{-i\gamma_i} z_i^*(\tau_i)\right\}\right]$$

- Rapid marginalisation over parameters other than sky location achieved via integral approximation and look-up tables.

- Result is a sky map probability density.

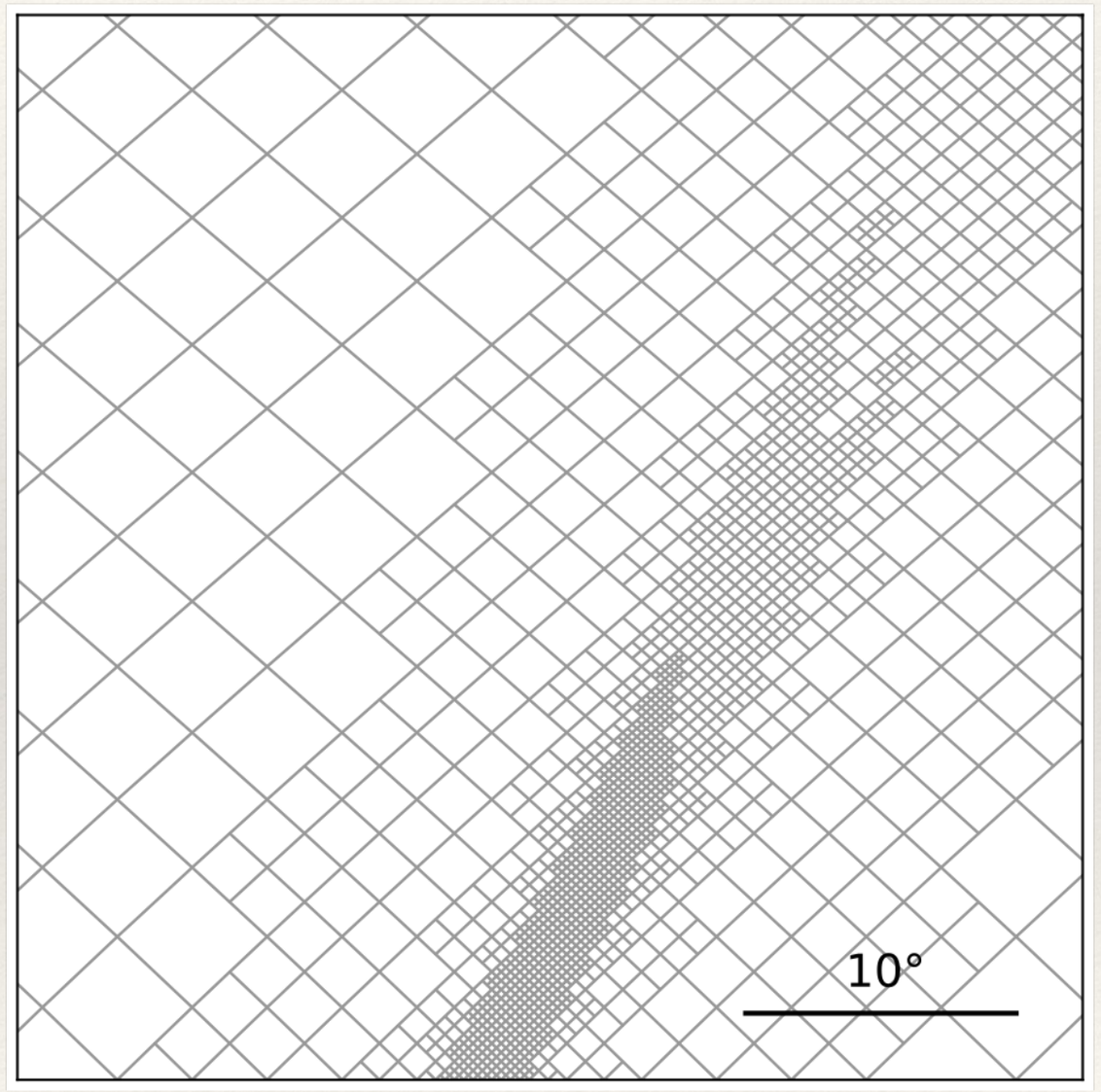

Singer & Price (2015)

Bayestar

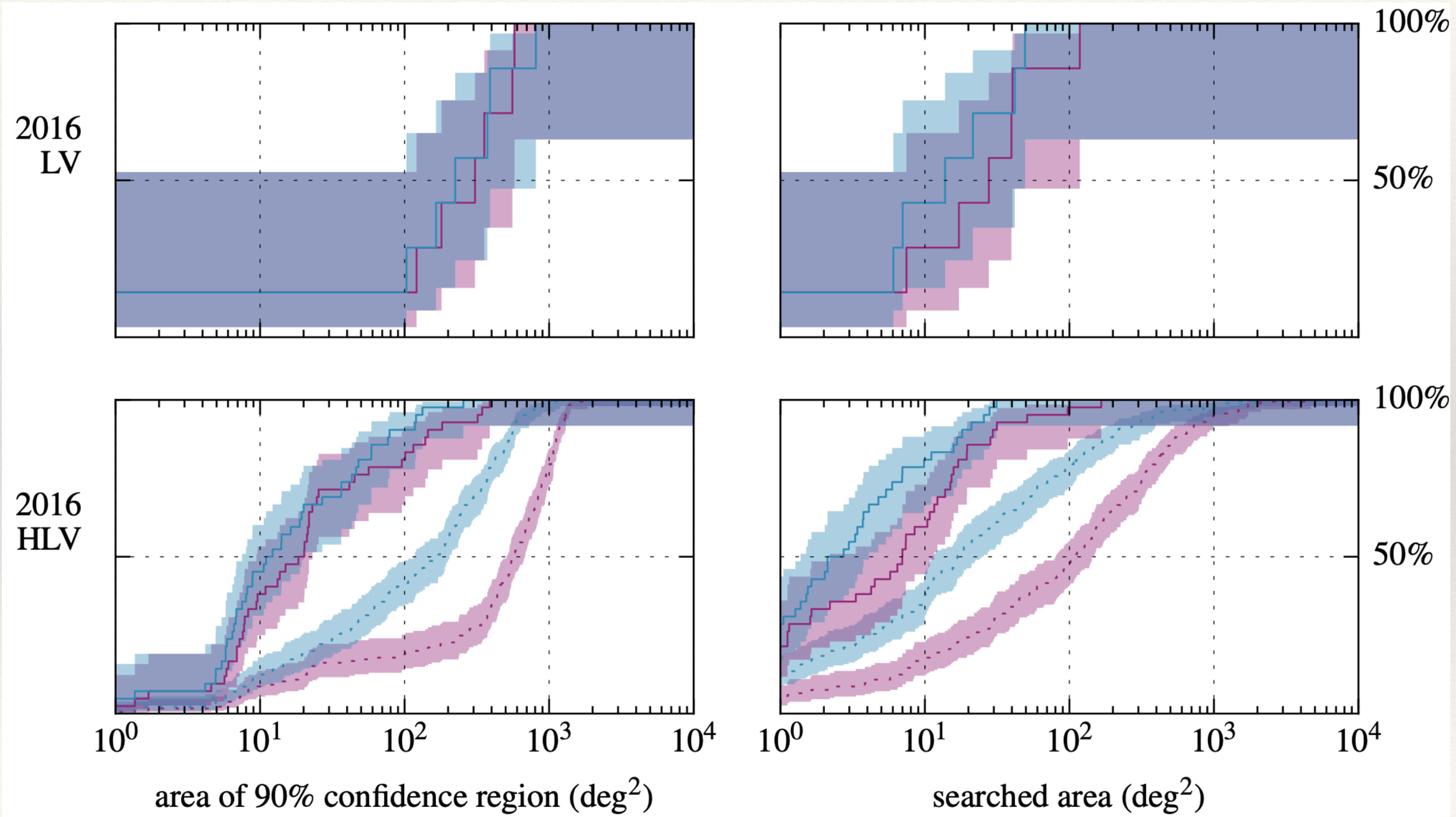

Singer & Price (2015)